Seeing the Sky

Visualization & Astronomers

David Spergel can change his mind.

Alyssa A. Goodman
Harvard Smithsonian Center for Astrophysics & Radcliffe Institute for Advanced Study
@aagie

HARVARD UNIVERSITY
Microsoft Research
NSF
SEAMLESS ASTRONOMY
Linking scientific data, publications, and communities
Authorea
NASA
AAS AMERICAN ASTRONOMICAL SOCIETY
Enhancing and sharing humanity's scientific understanding of the universe since 1899.

$$F = \frac{Gm_1m_2}{R^2}$$

Paper of the Future

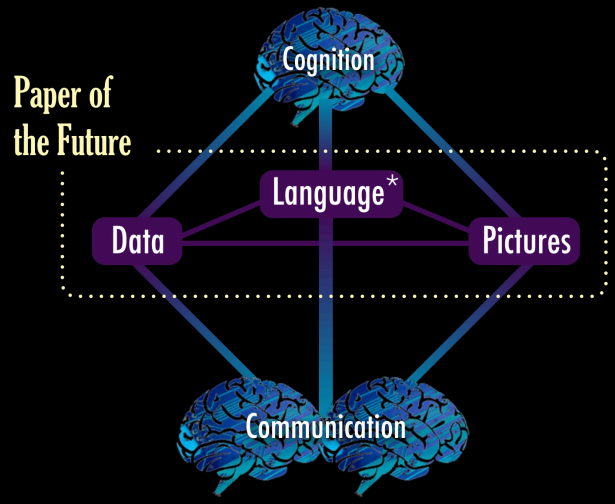

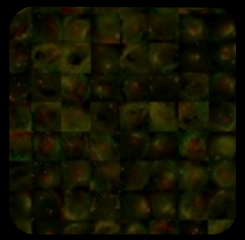

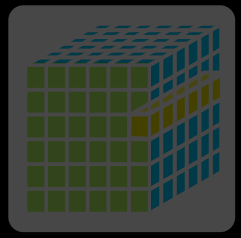

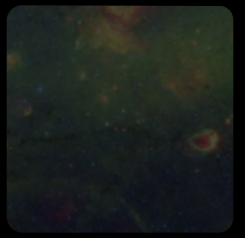

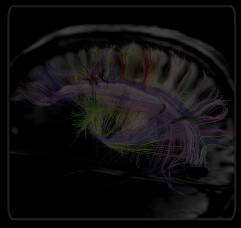

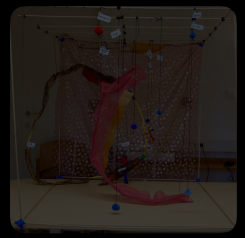

"Paper of the Future"

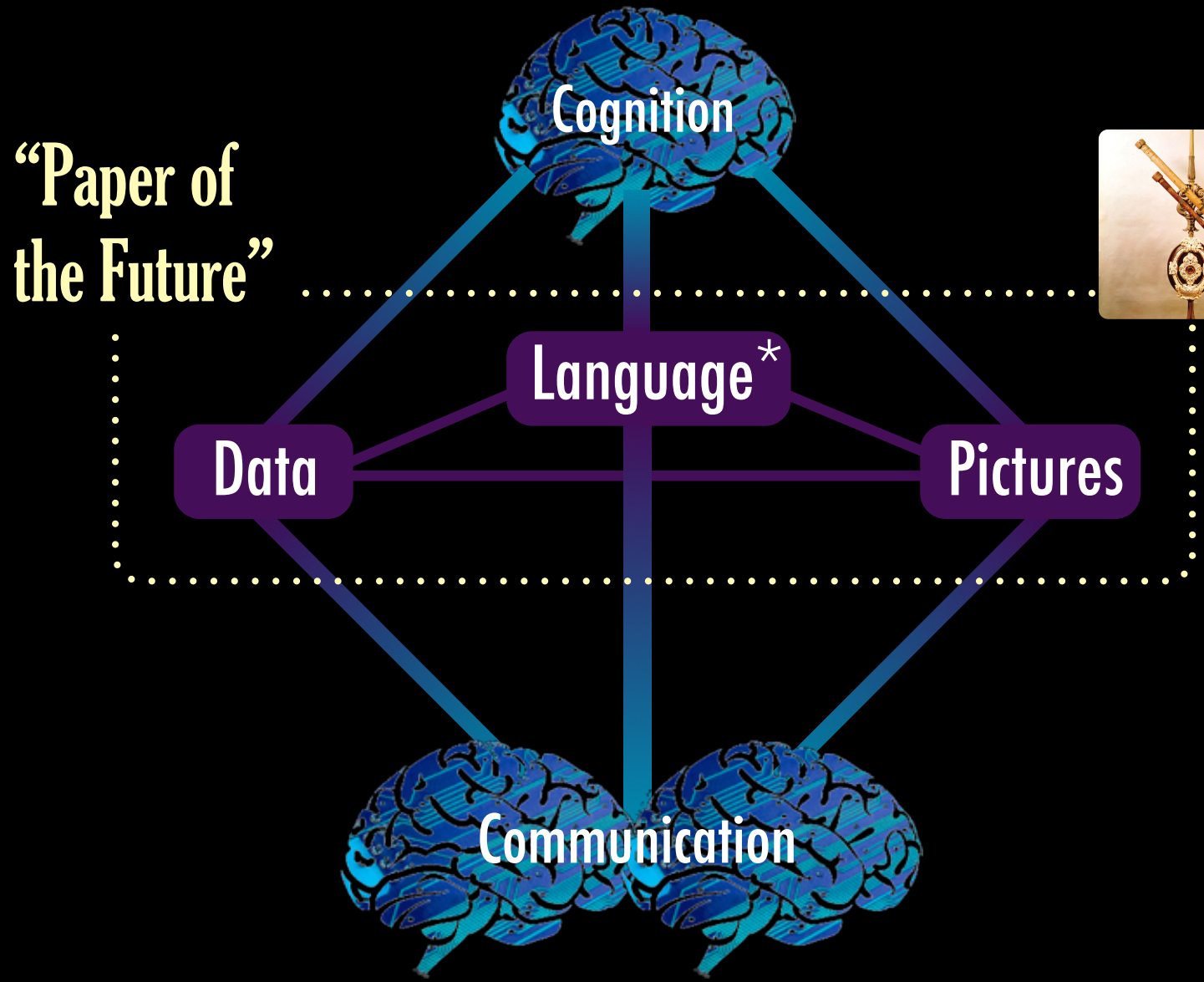

*"Language" includes words & math

Why Galileo is my Hero

Explore-Explain-Explore

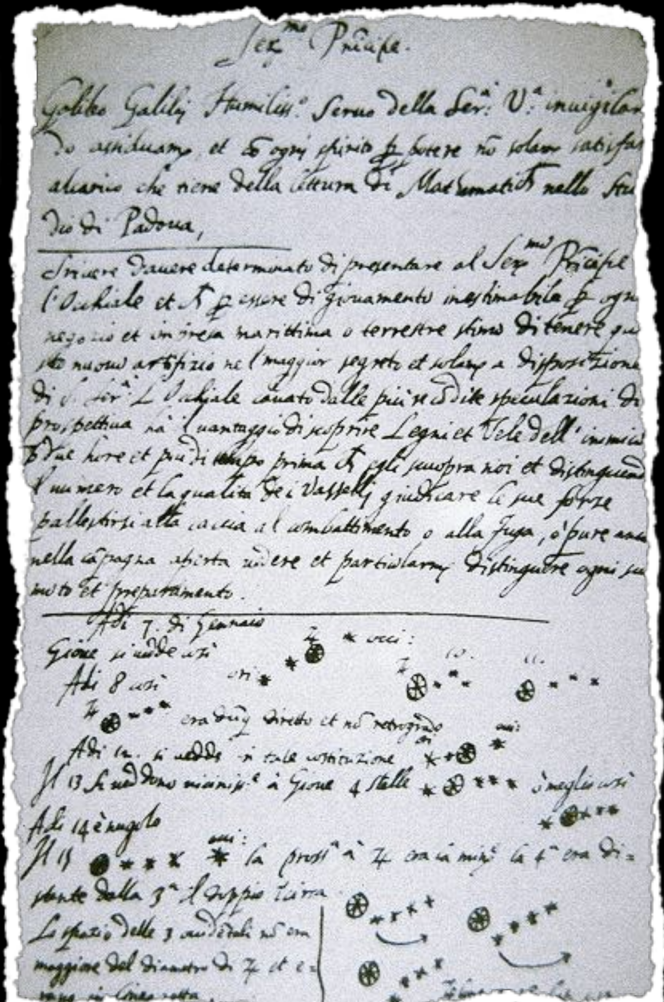

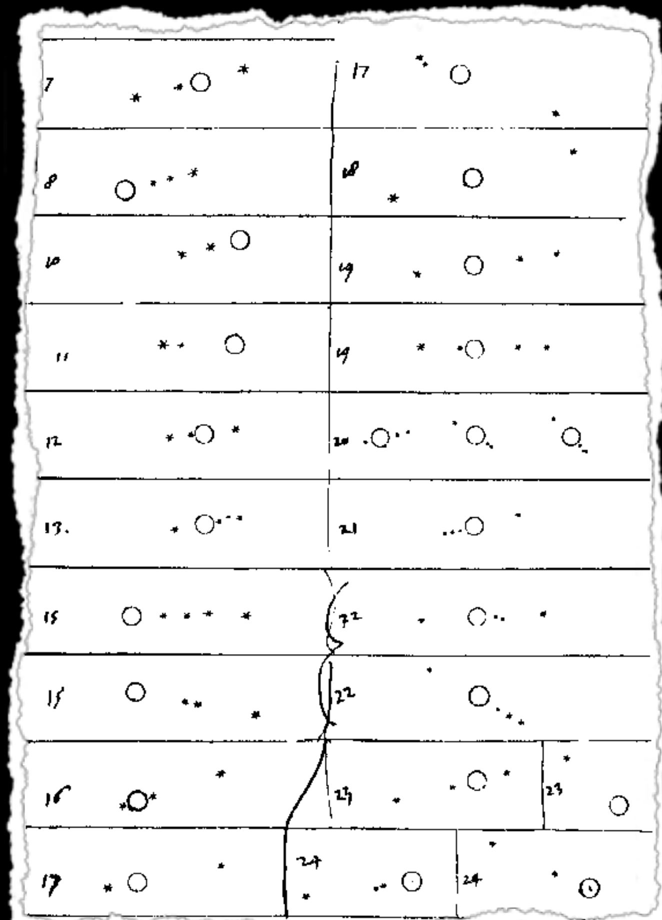

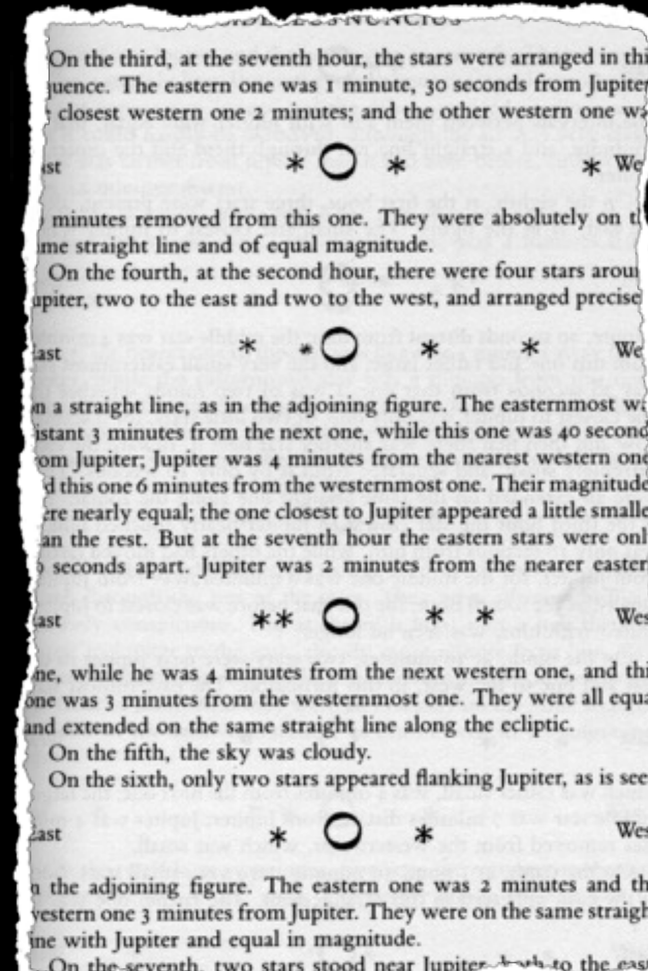
On the third, at the seventh hour, the stars were arranged in thi
quence. The eastern one was 1 minute, 30 seconds from Jupiter
closest western one 2 minutes; and the other western one w

ast * ○ * * We

minutes removed from this one. They were absolutely on t
me straight line and of equal magnitude.

On the fourth, at the second hour, there were four stars arou
upiter, two to the east and two to the west, and arranged precise

ast * *○ * * We

n a straight line, as in the adjoining figure. The easternmost w
istant 3 minutes from the next one, while this one was 40 second
om Jupiter; Jupiter was 4 minutes from the nearest western one
d this one 6 minutes from the westernmost one. Their magnitude
re nearly equal; the one closest to Jupiter appeared a little smalle
an the rest. But at the seventh hour the eastern stars were onl
seconds apart. Jupiter was 2 minutes from the nearer easter

ast ** ○ * * Wes

ne, while he was 4 minutes from the next western one, and thi
one was 3 minutes from the westernmost one. They were all equal
and extended on the same straight line along the ecliptic.

On the fifth, the sky was cloudy.

On the sixth, only two stars appeared flanking Jupiter, as is seen

ast * ○ * Wes

n the adjoining figure. The eastern one was 2 minutes and the
vestern one 3 minutes from Jupiter. They were on the same straigh
ine with Jupiter and equal in magnitude.

On the seventh, two stars stood near Jupiter, both to the east

Notes for & re-productions of Siderius Nuncius

1610

GALILEO'S "NEW ORDER"

Created by Alyssa Goodman, Curtis Wong and Pat Udomprasert,
with advice from Owen Gingerich and David Malin

Galileo's New Order, A WorldWide Telescope Tour by Goodman, Wong & Udomprasert 2010
WWT Software Wong (inventor, MS Research), Fay (architect, MS Reseearch), et al., now open source, hosted by AAS, Phil Rosenfield, Director
see wwtambassadors.org for more on WWT Outreach

January 11, 1610

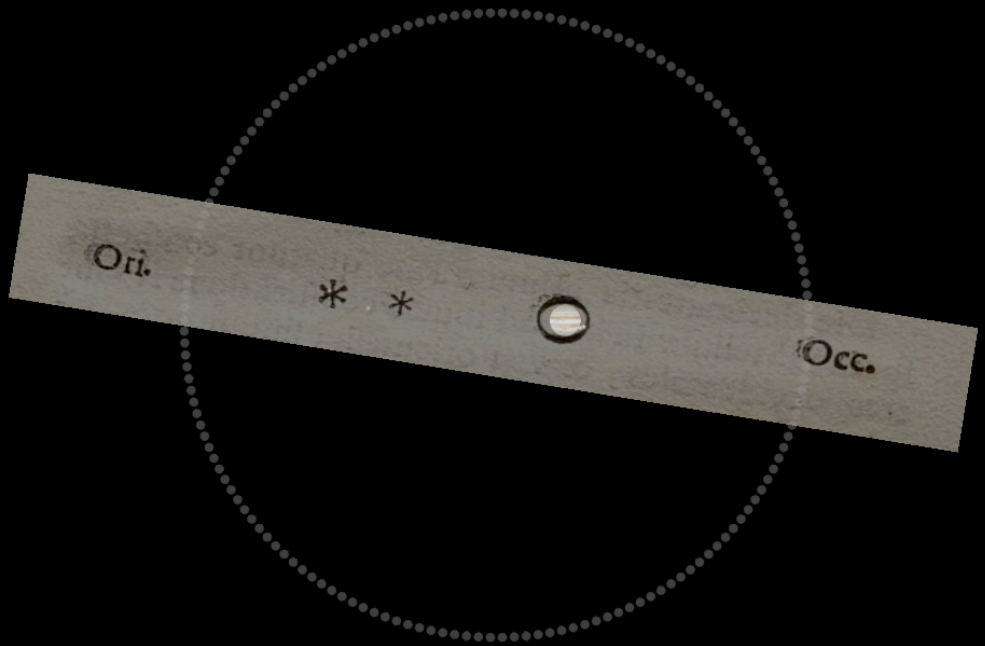

Galileo's New Order, A WorldWide Telescope Tour by Goodman, Wong & Udomprasert 2010
WWT Software Wong (inventor, MS Research), Fay (architect, MS Reseearch), et al., now open source, hosted by AAS, Phil Rosenfield, Director
see wwtambassadors.org for more on WWT Outreach

"Paper of the Future"

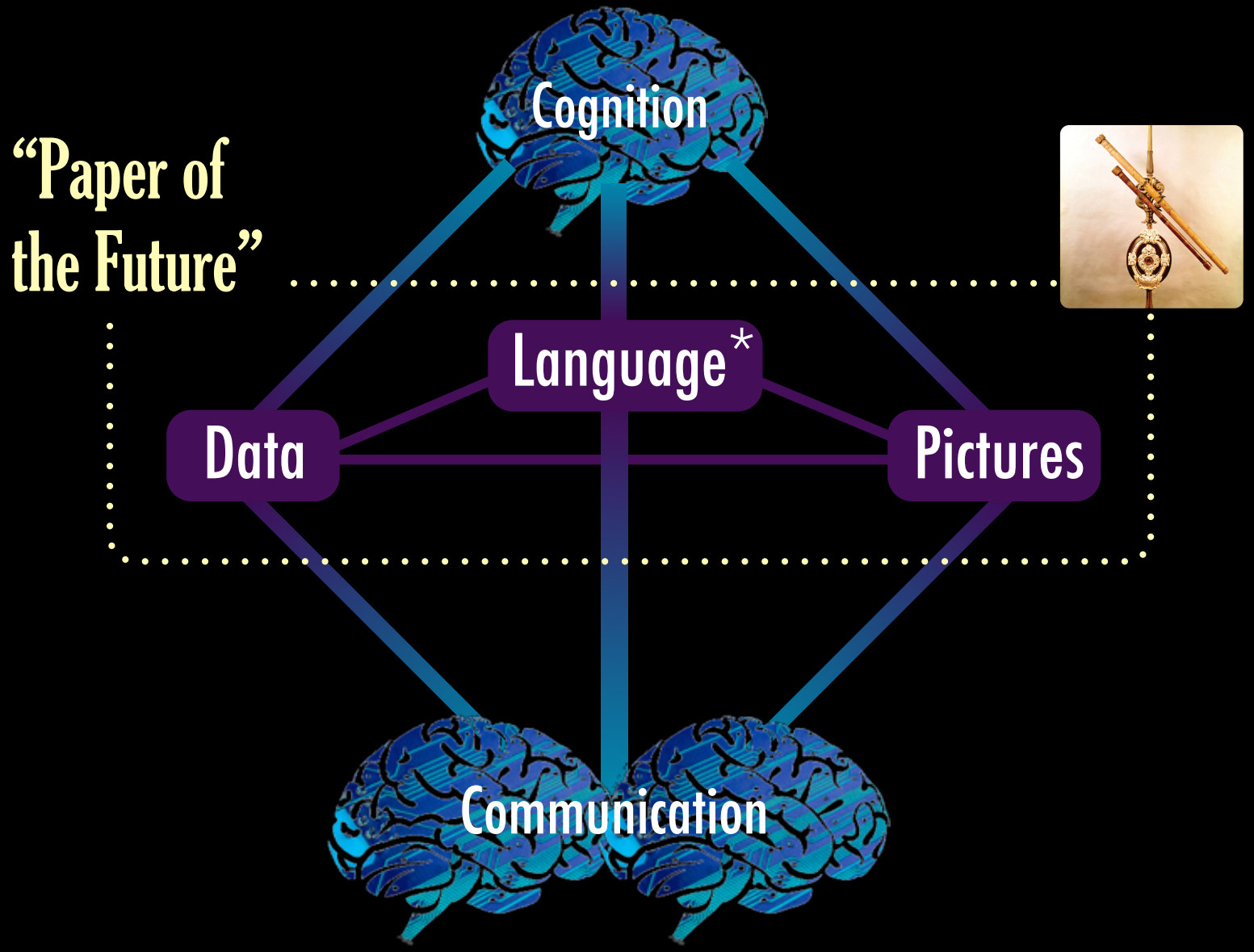

*"Language" includes words & math

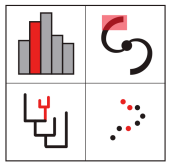

glue

multidimensional data exploration

enabled by d3.js (javascript) outputs

plotly

d3po

d3po is a project designed to allow an astronomer (or anyone), with no special data visualization skills, to make an interactive, publication-quality figure that has staged builds and linked brushing through scatter plots. Our current version can be previewed at d3po.org, and represents a figure from upcoming work by graduate student Elisabeth Newton. The figure describes how metallicity affects color in cool stars, and represents a nice use case for d3po. Try clicking and dragging in the scatter plots to understand the power of linked brushing in published figures.

Right now we are in search of alpha testers, who have figures that could be made interactive and who are willing to get their hands a little dirty (No javascript skills needed). In future versions, we plan to link to glue to allow the creation of d3po figures interactively. We are also exploring implementation of d3po within presentations and within authorea. Full 1.0 version expected in January 2014.

Installing your own d3po server

```
git clone git@github.com:adrn/d3po.git
cd d3po
virtualenv --no-site-packages venv
source venv/bin/activate
pip install -r pip-requirements.txt
python run.py
```

Authorea

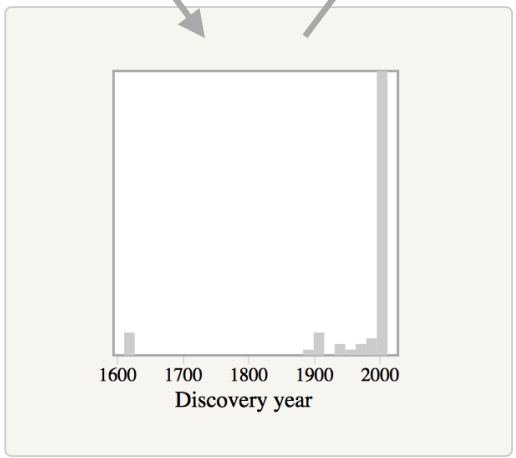

Four Centuries of Discovery | A Chasm in Mass | Little Siblings | Close Cousins | The Strangers

After Galileo discovered the first four moons of Jupiter, it took nearly three hundred years to discover the next one.

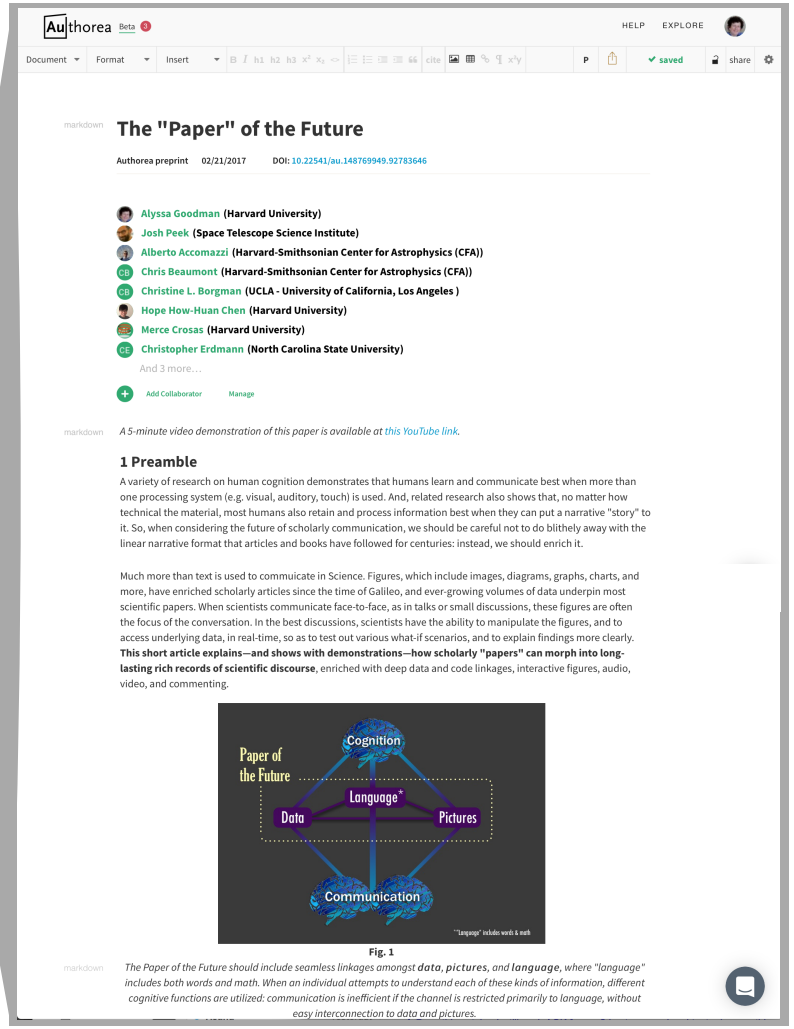

[demo]

Many thanks to Alberto Pepe, Josh Peek, Chris Beaumont, Tom Robitaille, Adrian Price-Whelan, Elizabeth Newton, Michelle Borkin & Matteo Cantiello for making this posible.

4 Centuries from Galileo to Galileo

1610

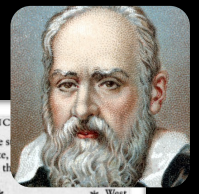

SIDEREUS NUNC

On the third, at the seventh hour, the s
sequence. The eastern one was 1 minute,
the closest western one 2 minutes; and th

East * ○ * * West

10 minutes removed from this one. They were absolutely on the
same straight line and of equal magnitude.

On the fourth, at the second hour, there were four stars around
Jupiter, two to the east and two to the west, and arranged precisely

East * *○ * * West

on a straight line, as in the adjoining figure. The easternmost was
distant 3 minutes from the next one, while this one was 40 seconds
from Jupiter; Jupiter was 4 minutes from the nearest western one,
and this one 6 minutes from the westernmost one. Their magnitudes
were nearly equal; the one closest to Jupiter appeared a little smaller
than the rest. But at the seventh hour the eastern s
30 seconds apart. Jupiter was 2 minutes from the

East ** ○ * *

one, while he was 4 minutes from the next western
one was 3 minutes from the westernmost one. They
and extended on the same straight line along the ec

On the fifth, the sky was cloudy.

On the sixth, only two stars appeared flanking Ju

East * ○ *

in the adjoining figure. The eastern one was 2 mi
western one 3 minutes from Jupiter. They were on th
line with Jupiter and equal in magnitude.

On the seventh, two stars stood near Jupiter, bo
arranged in this manner.

1665

PHILOSOPHICAL TRANSACTIONS

1895

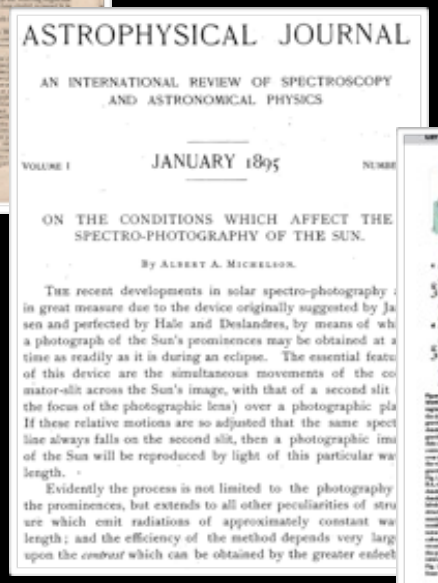

ASTROPHYSICAL JOURNAL

AN INTERNATIONAL REVIEW OF SPECTROSCOPY AND ASTRONOMICAL PHYSICS

VOLUME I JANUARY 1895 NUMBE

ON THE CONDITIONS WHICH AFFECT THE SPECTRO-PHOTOGRAPHY OF THE SUN.

By Albert A. Michelson.

The recent developments in solar spectro-photography
in great measure due to the device originally suggested by Ja
sen and perfected by Hale and Deslandres, by means of wh
a photograph of the Sun's prominences may be obtained at a
time as readily as it is during an eclipse. The essential featu
of this device are the simultaneous movements of the co
mator-slit across the Sun's image, with that of a second slit
the focus of the photographic lens) over a photographic pla
If these relative motions are so adjusted that the same spect
line always falls on the second slit, then a photographic ima
of the Sun will be reproduced by light of this particular wa
length.

Evidently the process is not limited to the photography
the prominences, but extends to all other peculiarities of stru
ure which emit radiations of approximately constant wa
length; and the efficiency of the method depends very larg
upon the *contrast* which can be obtained by the greater endeet

2009

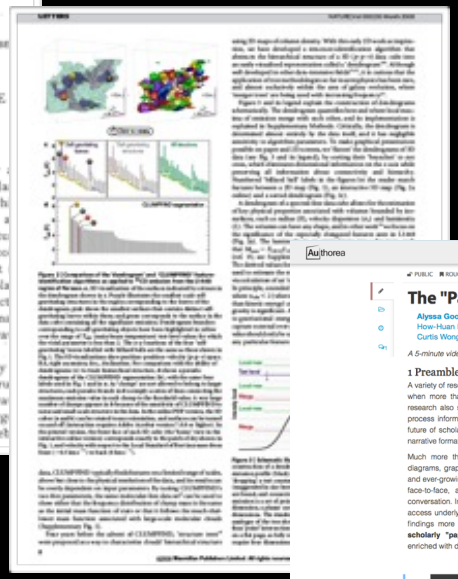

2015

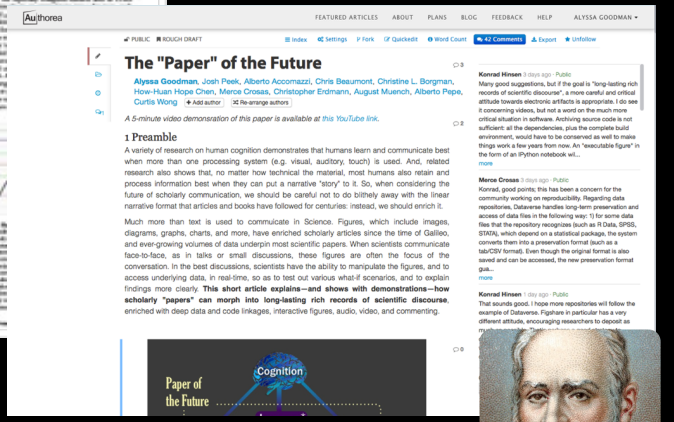

$$F = \frac{Gm_1m_2}{R^2}$$

Paper of the Future

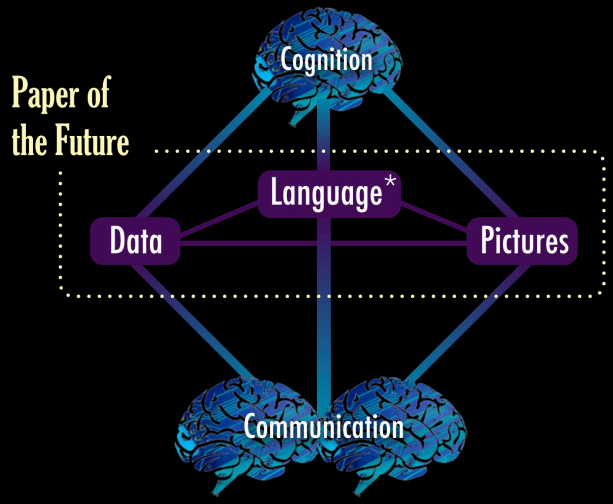

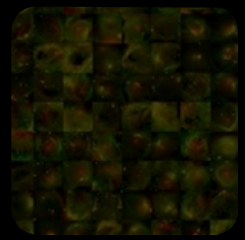

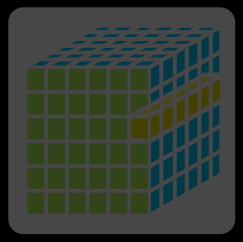

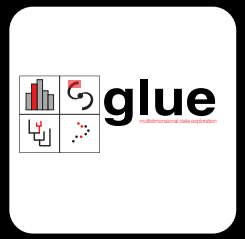

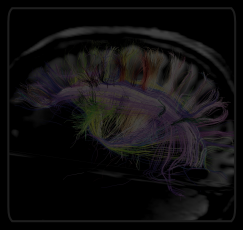

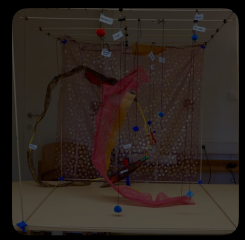

Big DATA
versus
Wide DATA

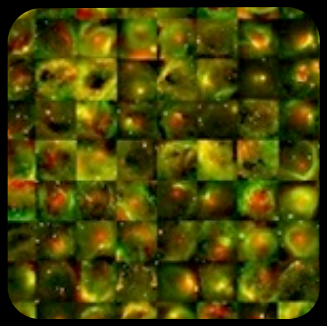

PHILOSOPHICAL
TRANSACTION

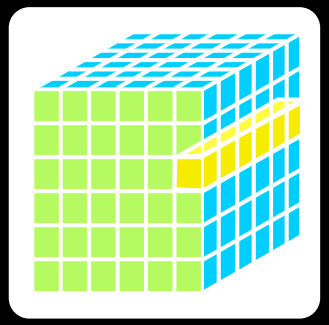

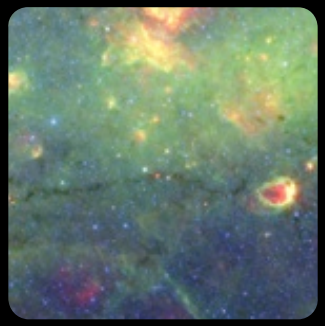

WorldWide Telescope

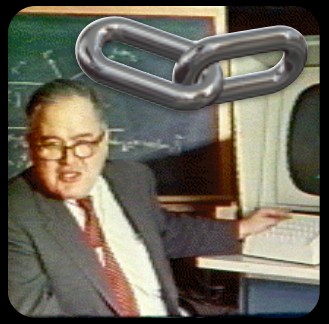

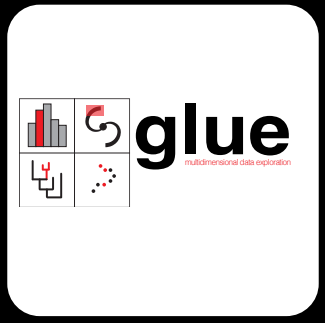
glue
multidimensional data exploration

ADS
ALL SKY
SURVEY

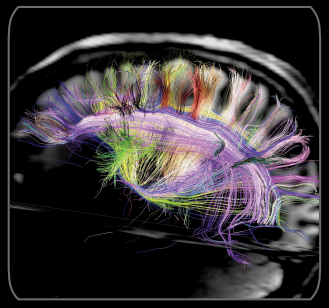

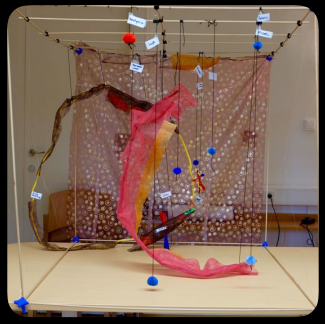

Big DATA
versus
Wide DATA

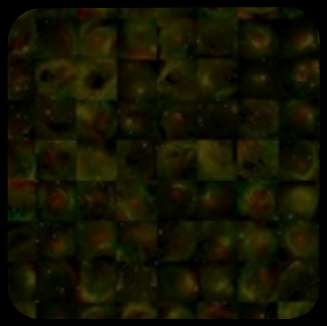

PHILOSOPHICAL
TRANSACTIONS

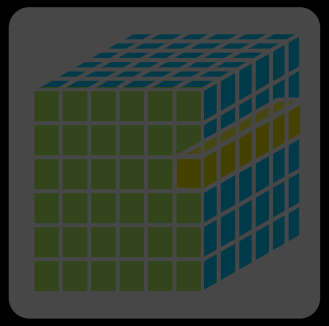

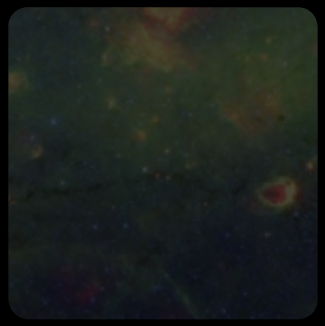

WorldWide Telescope

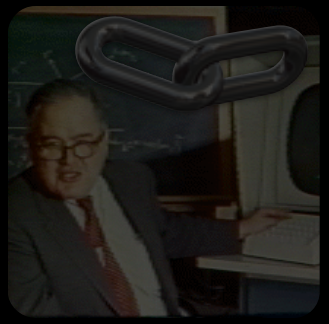

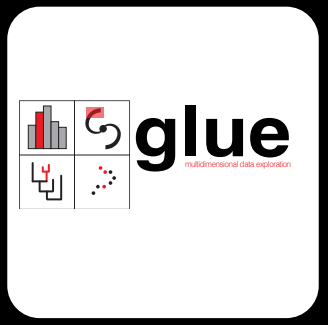
glue
multidimensional data exploration

ADS
ALL SKY
SURVEY

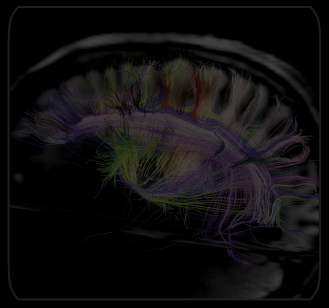

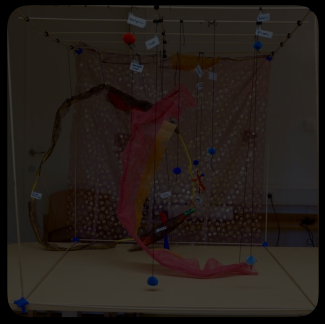

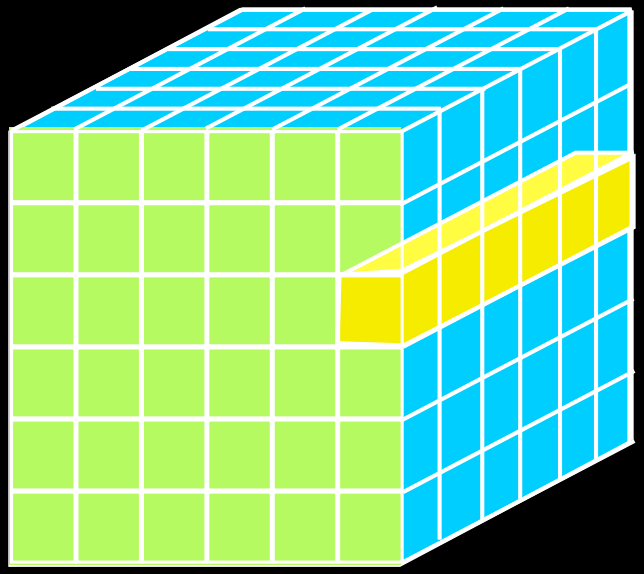

Data, Dimensions, Display

1D: Columns = “Spectra”, “SEDs” or “Time Series”
2D: Faces or Slices = “Images”
3D: Volumes = “3D Renderings”, “2D Movies”
4D: Time Series of Volumes = “3D Movies”

Data, Dimensions, Display

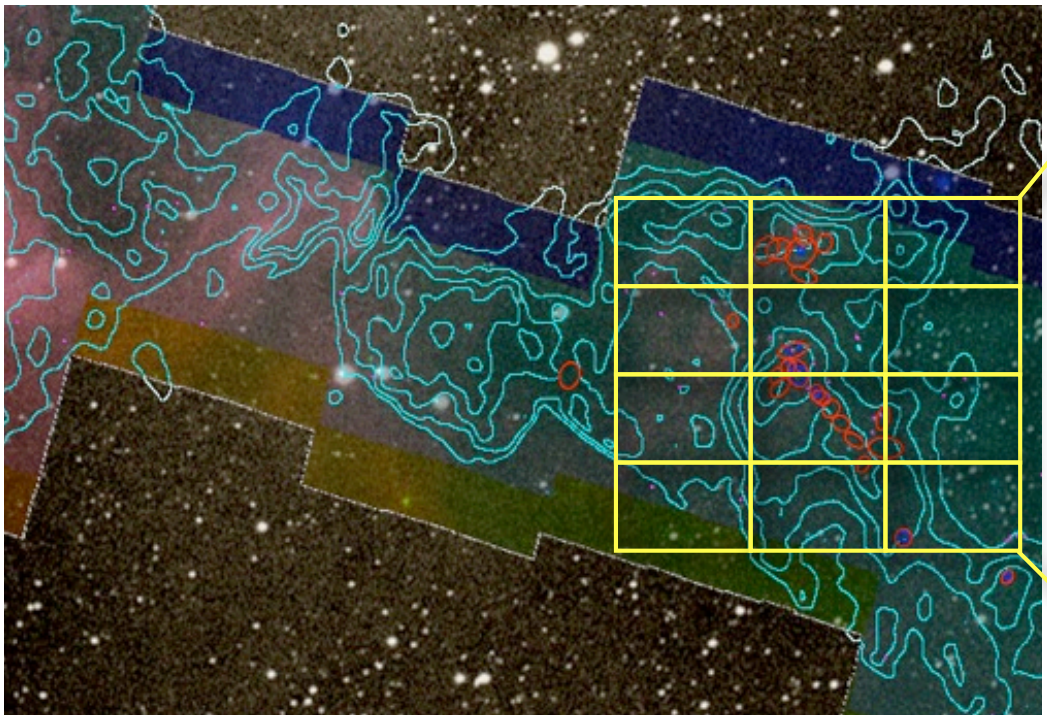

Spectral Line Observations

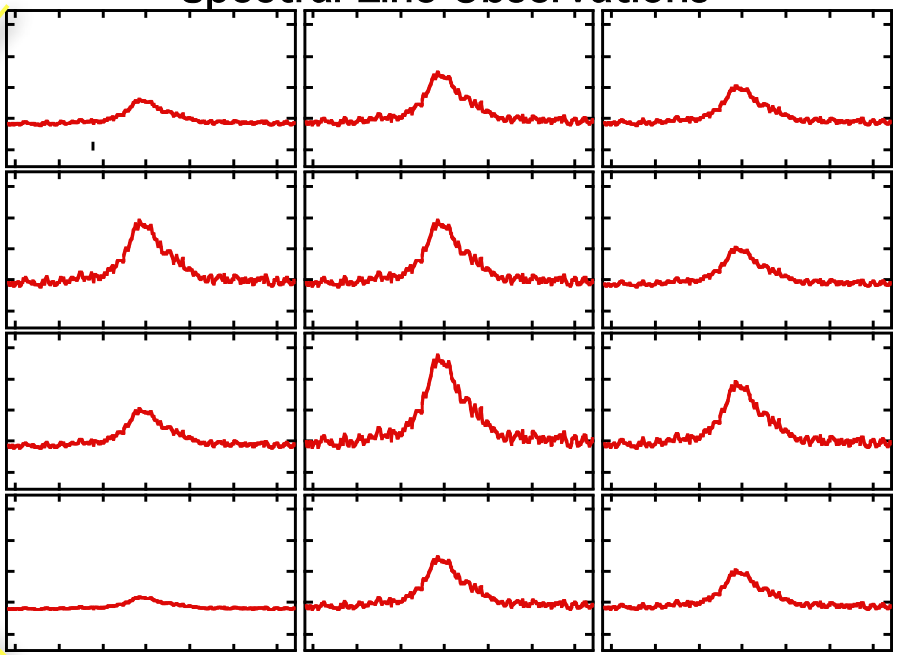

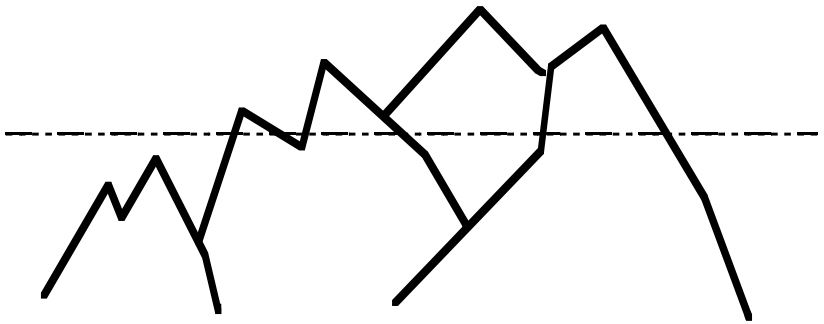

Mountain Range

No loss of information

Loss of 1 dimension

Data, Dimensions, Display

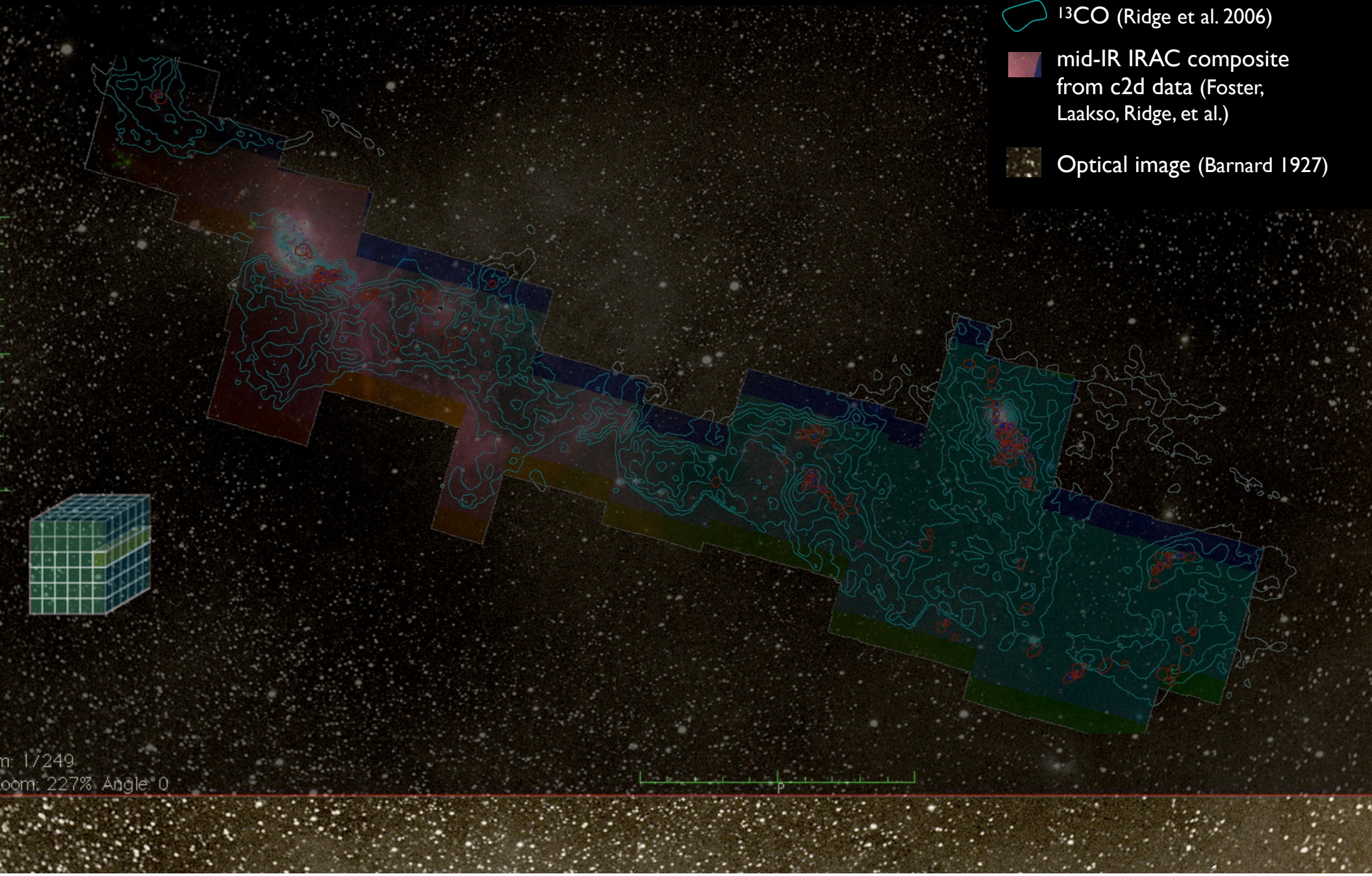

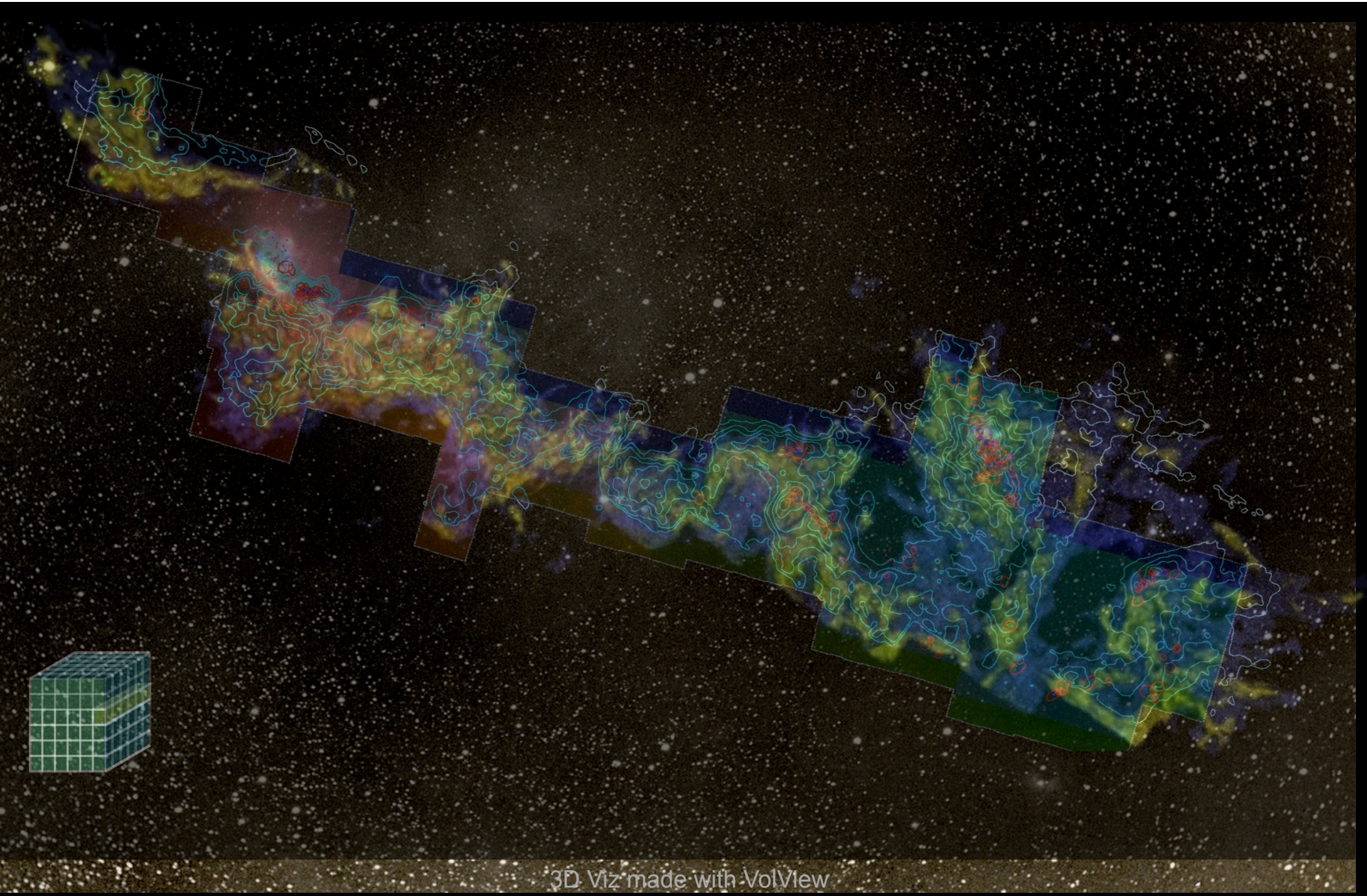

AstronomicalMedicine@IIG

COMPLETE

2009

3D PDF

High-Dimensional data in a "Paper" on its way to the Future

[demo/video]

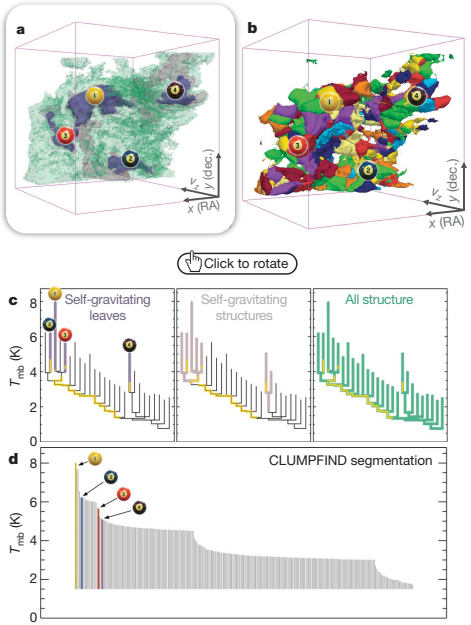

Figure 2 | Comparison of the 'dendrogram' and 'CLUMPFIND' feature-identification algorithms as applied to ^{13}CO emission from the L1448 region of Perseus. a, 3D visualization of the surfaces indicated by colours in the dendrogram shown in **c**. Purple illustrates the smallest scale self-gravitating structures in the region corresponding to the leaves of the dendrogram; pink shows the smallest surfaces that contain distinct self-gravitating leaves within them; and green corresponds to the surface in the data cube containing all the significant emission. Dendrogram branches corresponding to self-gravitating objects have been highlighted in yellow over the range of T_{mb} (main-beam temperature) test-level values for which the virial parameter is less than 2. The *x*–*y* locations of the four 'self-gravitating' leaves labelled with billiard balls are the same as those shown in Fig. 1. The 3D visualizations show position–position–velocity (*p*–*p*–*v*) space. RA, right ascension; dec., declination. For comparison with the ability of dendrograms (**c**) to track hierarchical structure, **d** shows a pseudo-dendrogram of the CLUMPFIND segmentation (**b**), with the same four labels used in Fig. 1 and in **a**. As 'clumps' are not allowed to belong to larger structures, each pseudo-branch in **d** is simply a series of lines connecting the maximum emission value in each clump to the threshold value. A very large number of clumps appears in **b** because of the sensitivity of CLUMPFIND to noise and small-scale structure in the data. In the online PDF version, the 3D cubes (**a** and **b**) can be rotated to any orientation, and surfaces can be turned on and off (interaction requires Adobe Acrobat version 7.0.8 or higher). In the printed version, the front face of each 3D cube (the 'home' view in the interactive online version) corresponds exactly to the patch of sky shown in Fig. 1, and velocity with respect to the Local Standard of Rest increases from front (-0.5 km s^{-1}) to back (8 km s^{-1}).

data, CLUMPFIND typically finds features on a limited range of scales, above but close to the physical resolution of the data, and its results can be overly dependent on input parameters. By tuning CLUMPFIND's two free parameters, the same molecular-line data set[8] can be used to show either that the frequency distribution of clump mass is the same as the initial mass function of stars or that it follows the much shallower mass function associated with large-scale molecular clouds (Supplementary Fig. 1).

Four years before the advent of CLUMPFIND, 'structure trees'[9] were proposed as a way to characterize clouds' hierarchical structure

using 2D maps of column density. With th…rly 2D work as inspiration, we have developed a structure-id…rithm that abstracts the hierarchical structure of a… an easily visualized representation calle… well developed in other data-intensive… application of tree methodologies so fa… and almost exclusively within the a… 'merger trees' are being used with in…

Figure 3 and its legend explain th… schematically. The dendrogram qua… ima of emission merge with each… explained in Supplementary Meth… determined almost entirely by th… sensitivity to algorithm paramet… possible on paper and 2D screen… data (see Fig. 3 and its legend… cross, which eliminates dimen… preserving all information… Numbered 'billiard ball' lab… features between a 2D map… online) and a sorted dendr…

A dendrogram of a spectr… of key physical properties… surfaces, such as radius (R), … (L). The volumes can have any shape, and… the significance of the especially elongated features… (Fig. 2a). The luminosity is an approximate proxy for mass, su… that $M_{lum} = X_{13CO} L_{13CO}$, where $X_{13CO} = 8.0 \times 10^{20}$ cm^2 K^{-1} km^{-1} s (ref. 15; see Supplementary Methods and Supplementary Fig. 2). The derived values for size, mass and velocity dispersion can then be used to estimate the role of self-gravity at each point in the hierarchy, via calculation of an 'observed' virial parameter, $\alpha_{obs} = 5\sigma_v^2 R/GM_{lum}$. In principle, extended portions of the tree (Fig. 2, yellow highlighting) where $\alpha_{obs} < 2$ (where gravitational energy is comparable to or larger than kinetic energy) correspond to regions of *p*–*p*–*v* space where self-gravity is significant. As α_{obs} only represents the ratio of kinetic energy to gravitational energy at one point in time, and does not explicitly capture external over-pressure and/or magnetic fields[16], its measured value should only be used as a guide to the longevity (boundedness) of any particular feature.

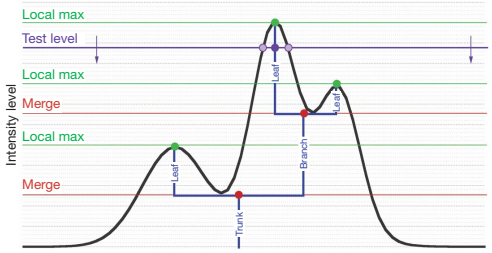

Figure 3 | Schematic illustration of the dendrogram process. Shown is the construction of a dendrogram from a hypothetical one-dimensional emission profile (black). The dendrogram (blue) can be constructed by 'dropping' a test constant emission level (purple) from above in tiny steps (exaggerated in size here, light lines) until all the local maxima and mergers are found, and connected as shown. The intersection of a test level with the emission is a set of points (for example the light purple dots) in one dimension, a planar curve in two dimensions, and an isosurface in three dimensions. The dendrogram of 3D data shown in Fig. 2c is the direct analogue of the tree shown here, only constructed from 'isosurface' rather than 'point' intersections. It has been sorted and flattened for representation on a flat page, as fully representing dendrograms for 3D data cubes would require four dimensions.

©2009 Macmillan Publishers Limited. All rights reserved

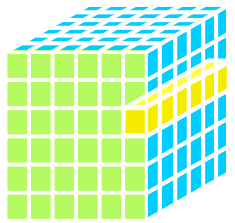

Goodman et al. 2009, Nature, cf: Fluke et al. 2009

Create | 1 / 4 | 131% | Tools | Comment | Share

Vol 457|1 January 2009|doi:10.1038/nature07609 nature

LETTERS

A role for self-gravity at multiple length scales in the process of star formation

Alyssa A. Goodman[1,2], Erik W. Rosolowsky[2,3], Michelle A. Borkin[1]†, Jonathan B. Foster[2], Michael Halle[1,4], Jens Kauffmann[1,2] & Jaime E. Pineda[2]

Self-gravity plays a decisive role in the final stages of star formation, where dense cores (size ~0.1 parsecs) inside molecular clouds collapse to form star-plus-disk systems[1]. But self-gravity's role at earlier times (and on larger length scales, such as ~1 parsec) is unclear; some molecular cloud simulations that do not include self-gravity suggest that 'turbulent fragmentation' alone is sufficient to create a mass distribution of dense cores that resembles, and sets, the stellar initial mass function[2]. Here we report a 'dendrogram' (hierarchical tree-diagram) analysis that reveals that self-gravity plays a significant role over the full range of possible scales traced by ^{13}CO observations in the L1448 molecular cloud, but not everywhere in the observed region. In particular, more than 90 per cent of the compact 'pre-stellar cores' traced by peaks of dust emission[3] are projected on the sky within one of the dendrogram's self-gravitating 'leaves'. As these peaks mark the locations of already-forming stars, or of those probably about to form, a self-gravitating cocoon seems a critical condition for their exist-

overlapping features as an option, significant emission found between prominent clumps is typically either appended to the nearest clump or turned into a small, usually 'pathological', feature needed to encompass all the emission being modelled. When applied to molecular-line

Why AstronomicalMedicine?

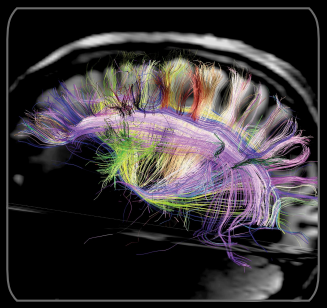

"KEITH"

"PERSEUS"

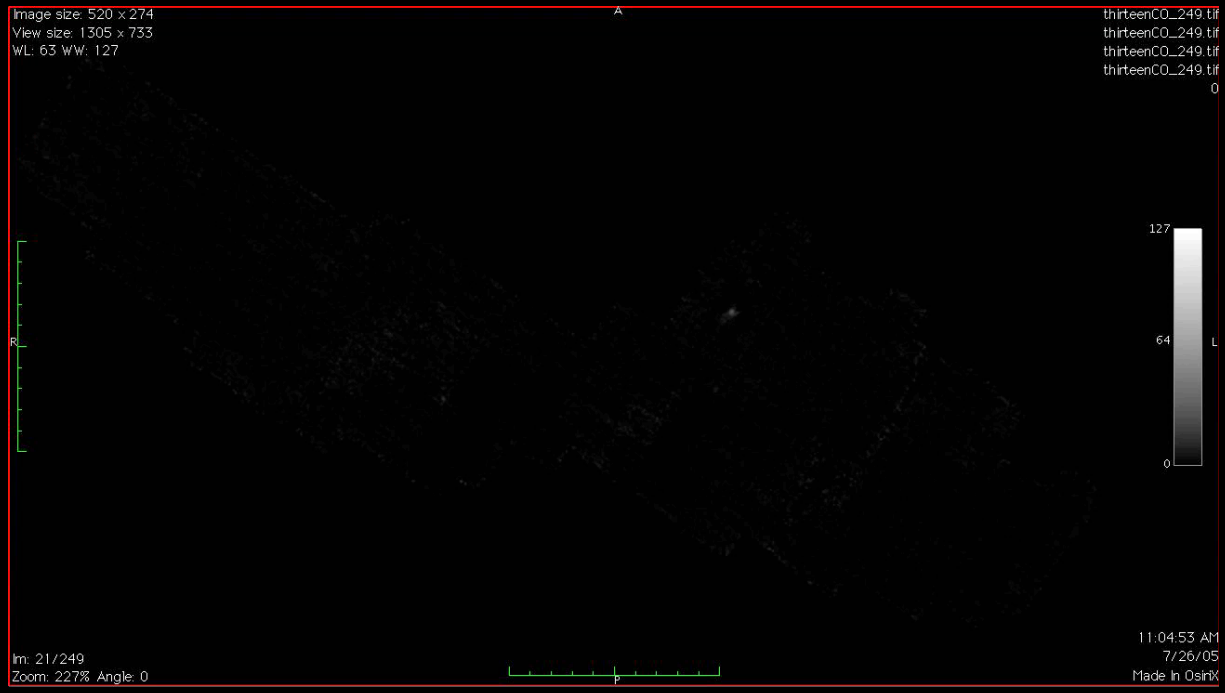

"z" is depth into head

"z" is line-of-sight velocity

Why AstronomicalMedicine?

chandra.harvard.edu/photo/2014/m106/

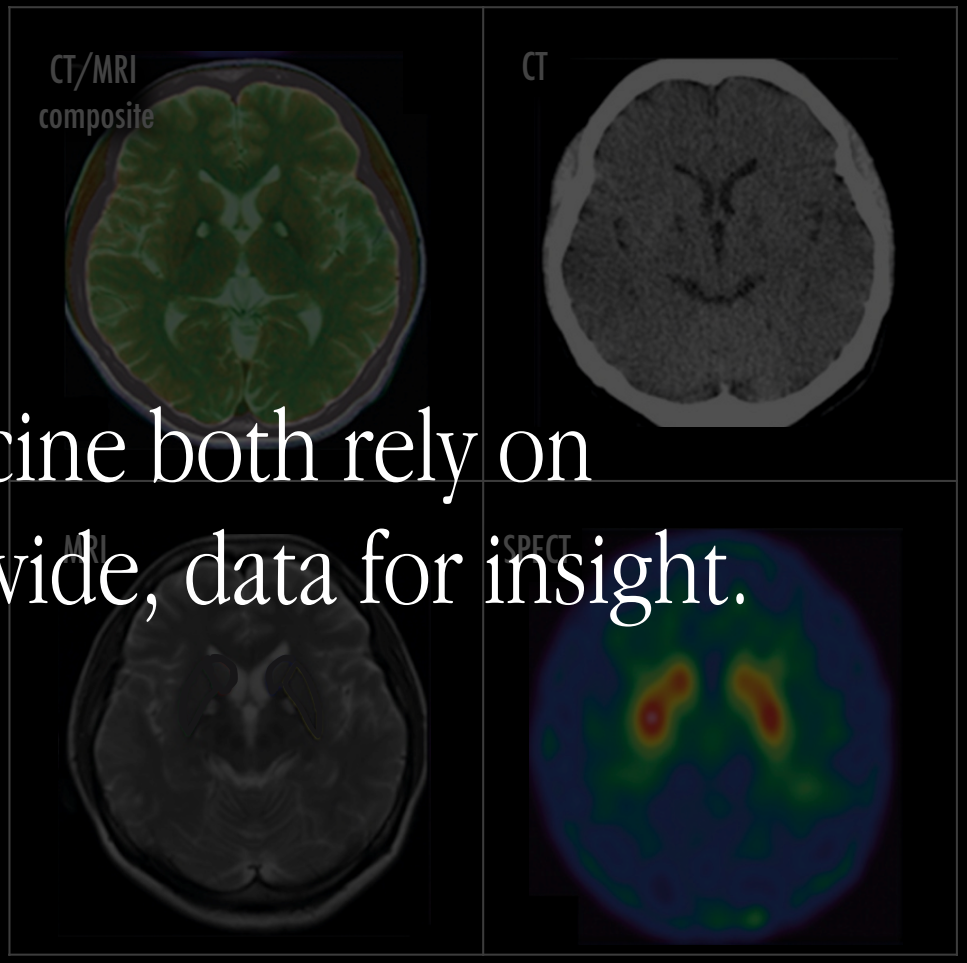

Chang, et al. 2011, brain.oxfordjournals.org/content/134/12/3632

Astronomy & Medicine both rely on high-dimensional, big, wide, data for insight.

Big DATA versus Wide DATA

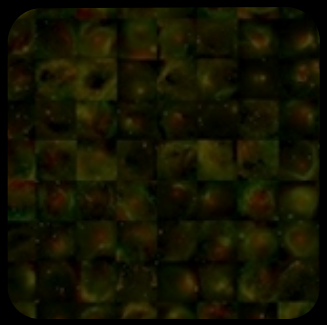

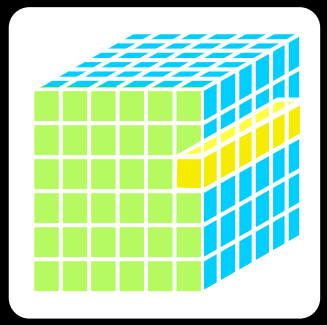

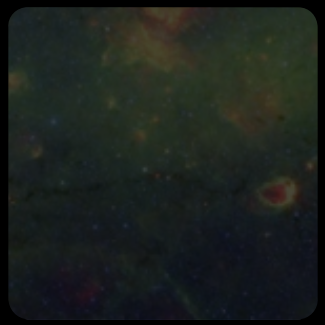

glue
multidimensional data exploration

ADS ALL SKY SURVEY

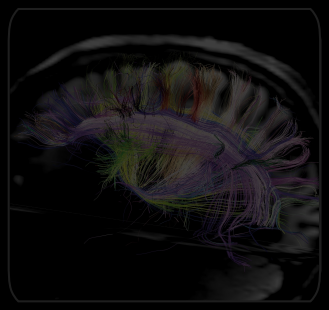

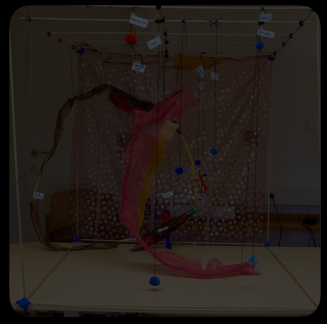

WIDE DATA

Big DATA versus Wide DATA

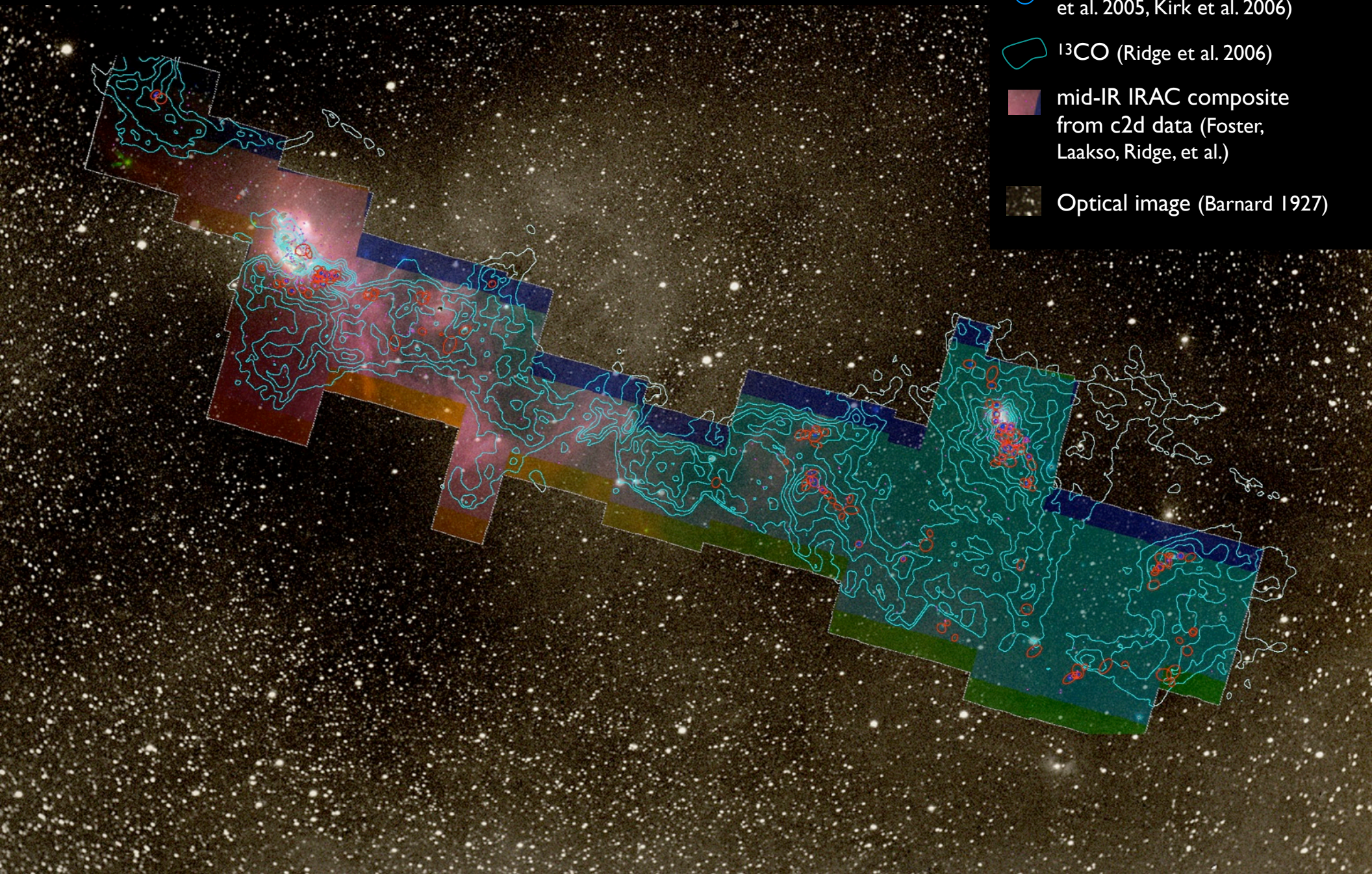

WIDE DATA

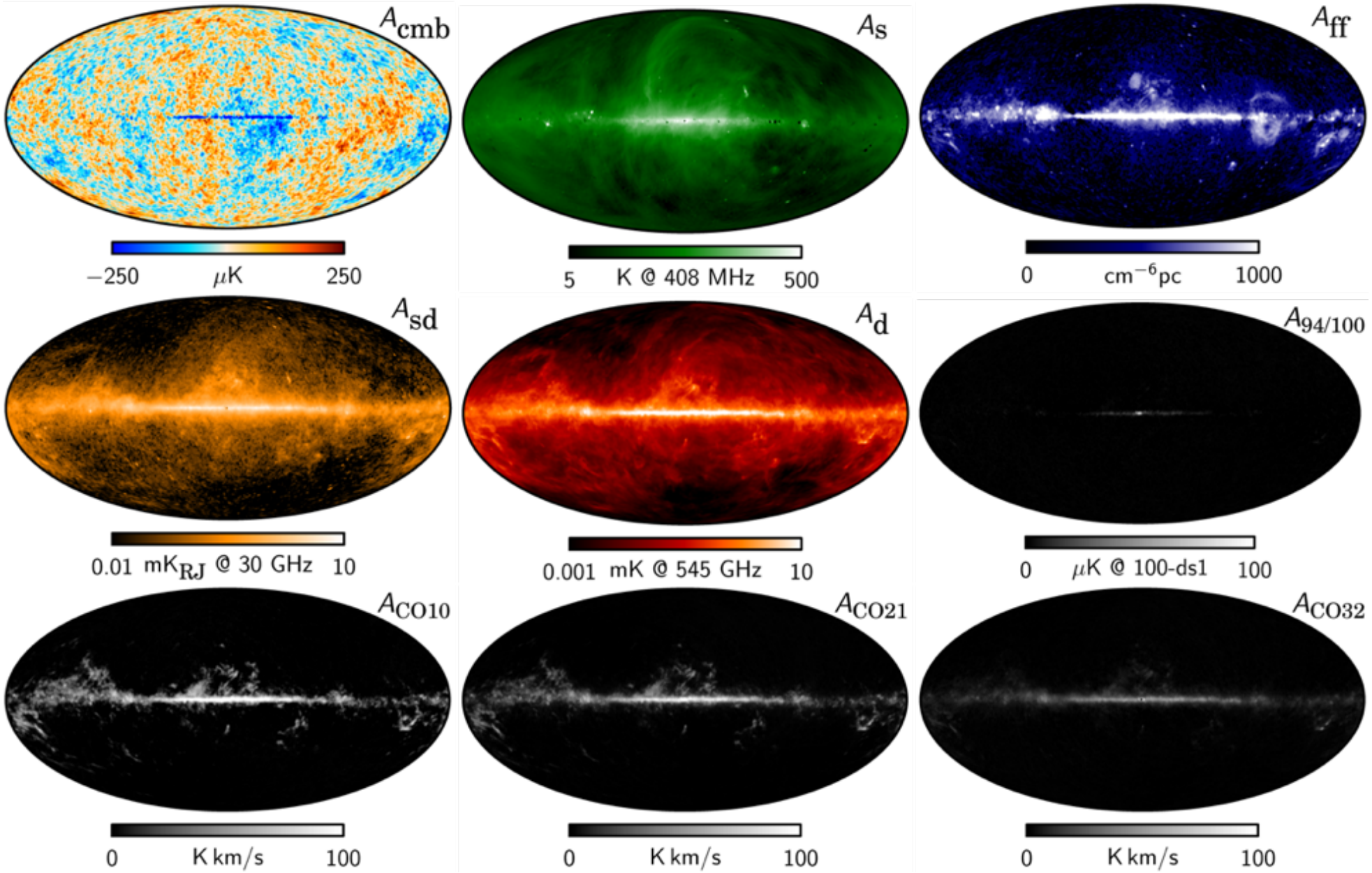

Temperature Foreground amplitudes from Commander, Planck Data [Feb 2015]

Explore
Guided Tours
Search
View
Settings
Install Windows Client
Use Layer Manager to Control User Settings
Name My Location
Lat 37:47:15
Alt 0 m
Lng -123:35:23
View From This Location
2015/02/11 04:40:33
Real Time
Now
Galactic Plane Mode
Big DATA versus Wide DATA
WorldWide Telescope
ZOONIVERSE
BIG DATA
Look At
Sky
Imagery
Digitized Sky Survey (Color)
Image Crossfade
Tracking
GLIMPSE/MIPSGAL
1 of 3
N
Scorpius
RA: 17h28m14s
Pismis 24 and
NGC6334
NGC6357
NGC6374
NGC6383
NGC6396
NGC6404
Lesath
Shaula
HR6397
HR6405

BIG DATA AND "HUMAN-AIDED COMPUTING"

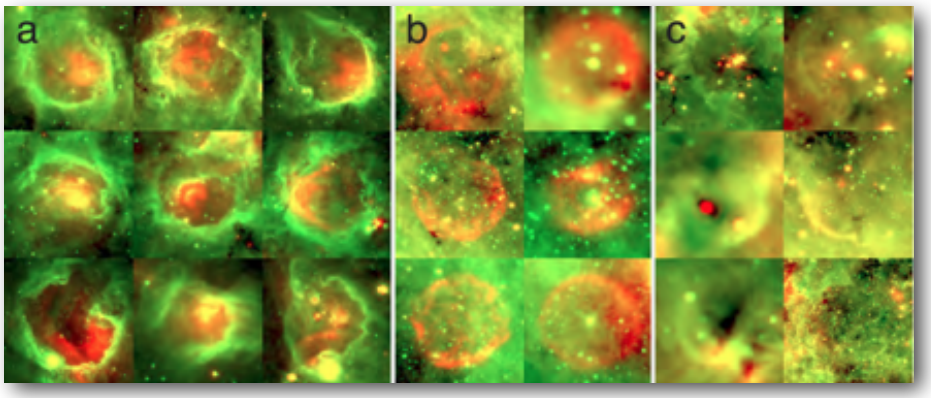

machine-learning algorithm (Brut)

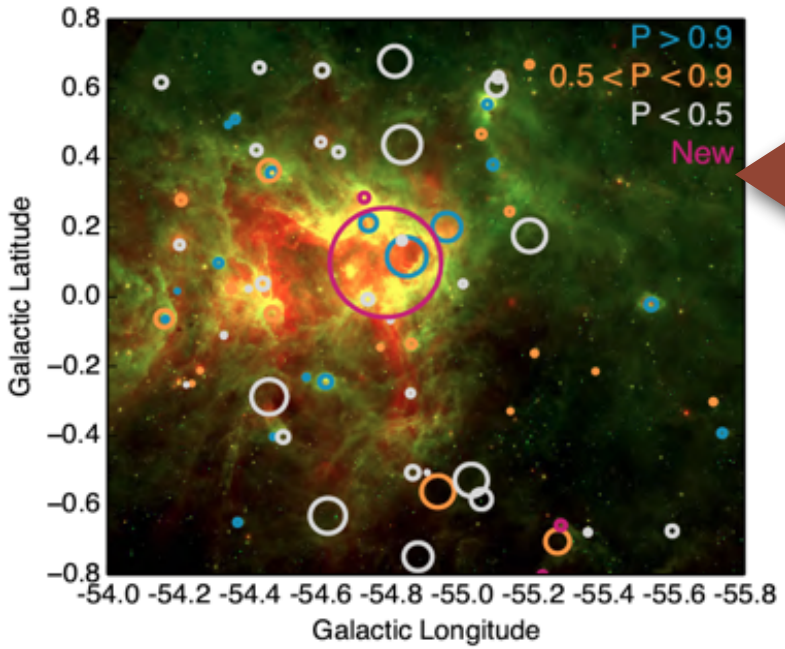

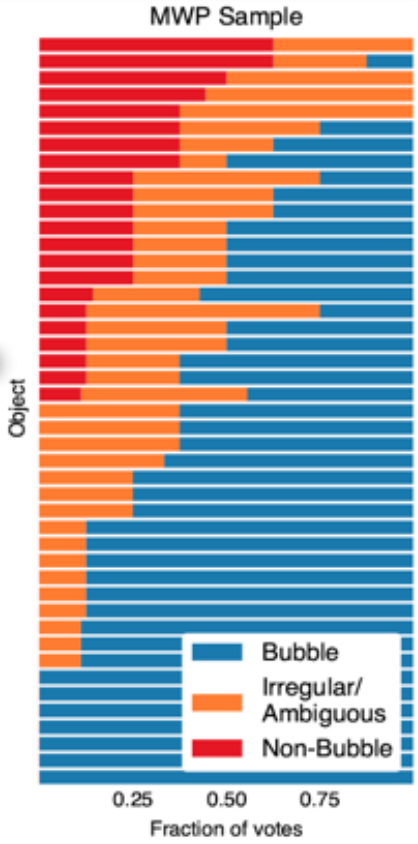

example here from: ***Beaumont****, Goodman, Kendrew, Williams & Simpson 2014; based on* ***Milky Way Project*** *catalog (Simpson et al. 2013), which came from* ***Spitzer/GLIMPSE*** *(Churchwell et al. 2009, Benjamin et al. 2003), cf. Shenoy & Tan 2008 for discussion of HAC;* ***astroml.org*** *for machine learning advice/tools*

BIG DATA AND "HUMAN-AIDED COMPUTING"

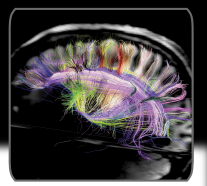

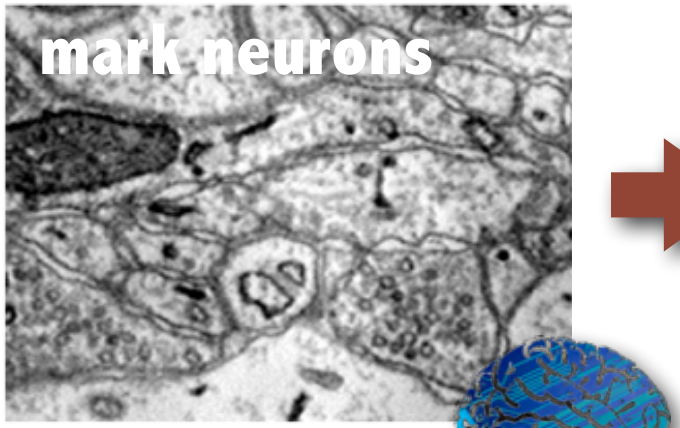

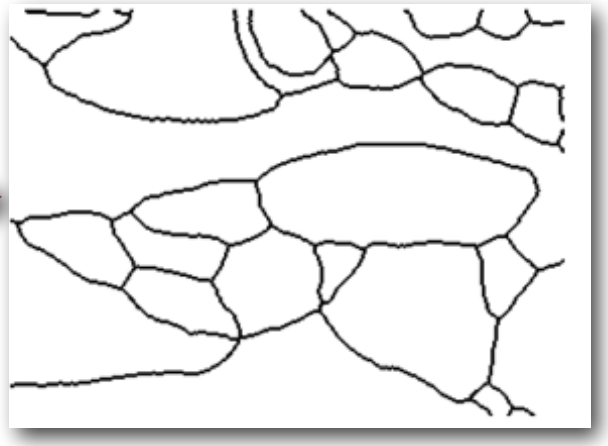

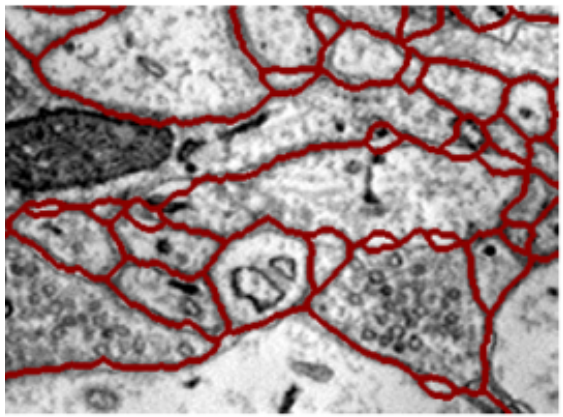

machine-learning algorithm (RF+CRF)

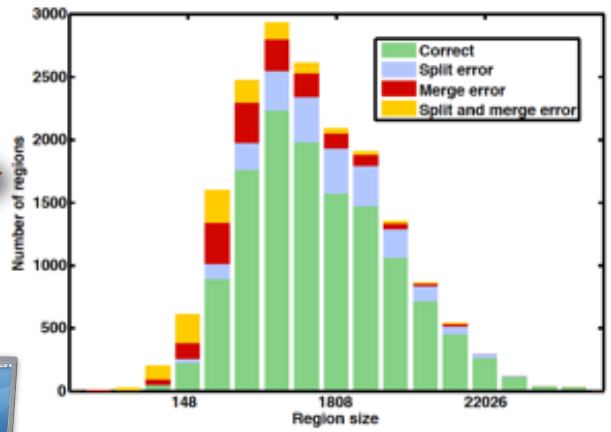

example here from: Kaynig...Lichtman...Pfister et al. 2013, "Large-Scale Automatic Reconstruction of Neuronal Processes from Electron Microscopy Images"; cf. Shenoy & Tan 2008 for discussion of HAC; ***astroml.org*** *for machine learning advice/tools (Note: RF=Random Forest; CRF=Conditional Random Fields.)*

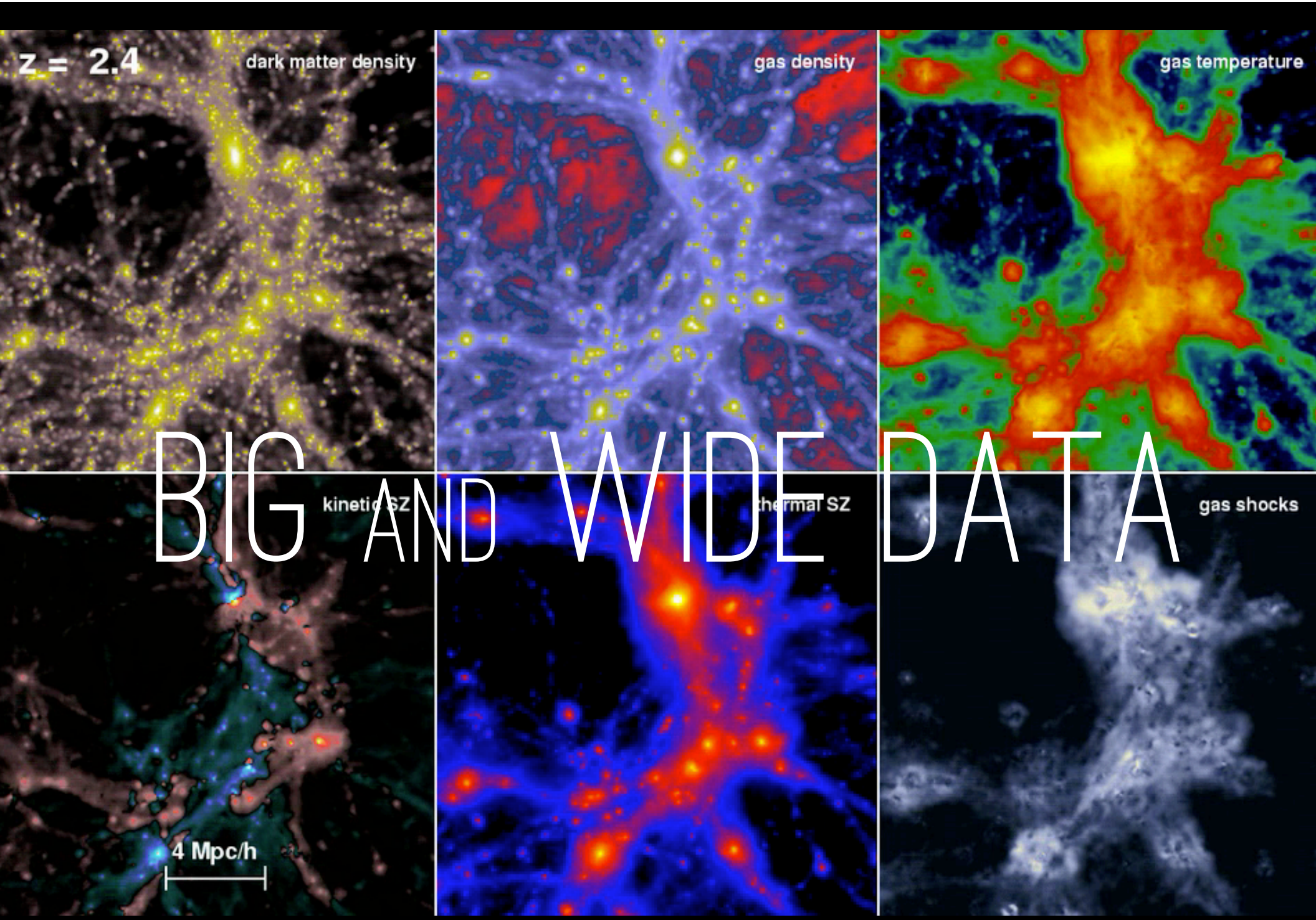

BIG AND WIDE DATA

Movie: Volker Springel, formation of a cluster of galaxies. Millenium Simulation requires 25TB for output.

Big DATA versus Wide DATA

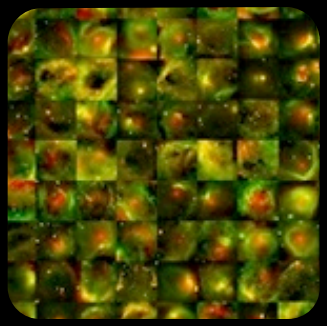

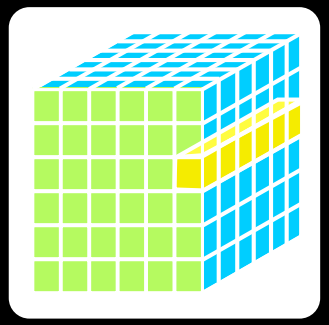

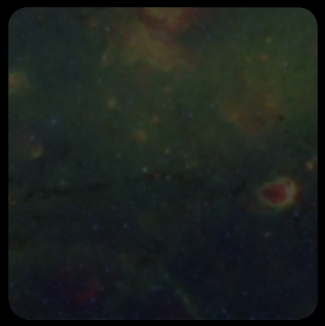

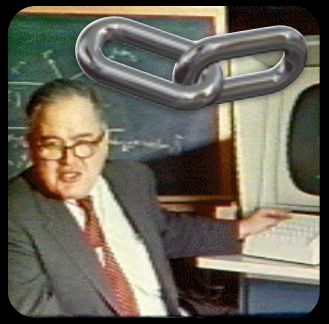

glue
multidimensional data exploration

ADS ALL SKY SURVEY

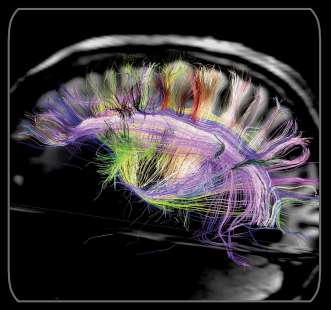

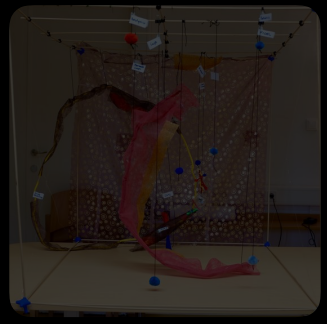

2009

3D PDF

High-Dimensional data in a "Paper" on its way to the Future

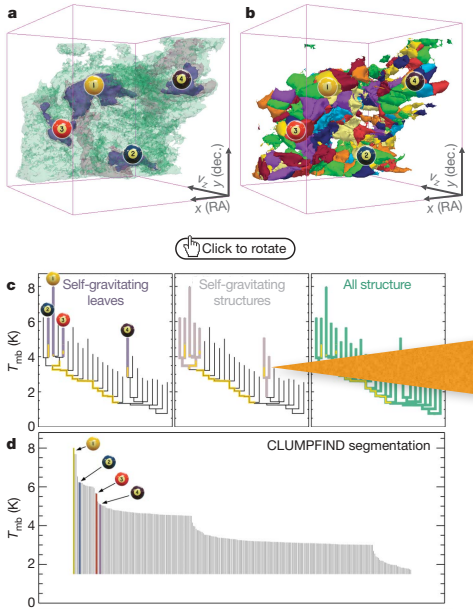

Figure 2 | Comparison of the 'dendrogram' and 'CLUMPFIND' feature-identification algorithms as applied to ^{13}CO emission from the L1448 region of Perseus. a, 3D visualization of the surfaces indicated by colours in the dendrogram shown in **c**. Purple illustrates the smallest scale self-gravitating structures in the region corresponding to the leaves of the dendrogram; pink shows the smallest surfaces that contain distinct self-gravitating leaves within them; and green corresponds to the surface in the data cube containing all the significant emission. Dendrogram branches corresponding to self-gravitating objects have been highlighted in yellow over the range of T_{mb} (main-beam temperature) test-level values for which the virial parameter is less than 2. The x–y locations of the four 'self-gravitating' leaves labelled with billiard balls are the same as those shown in Fig. 1. The 3D visualizations show position–position–velocity (p–p–v) space. RA, right ascension; dec., declination. For comparison with the ability of dendrograms (**c**) to track hierarchical structure, **d** shows a pseudo-dendrogram of the CLUMPFIND segmentation (**b**), with the same four labels used in Fig. 1 and in **a**. As 'clumps' are not allowed to belong to larger structures, each pseudo-branch in **d** is simply a series of lines connecting the maximum emission value in each clump to the threshold value. A very large number of clumps appears in **b** because of the sensitivity of CLUMPFIND to noise and small-scale structure in the data. In the online PDF version, the 3D cubes (**a** and **b**) can be rotated to any orientation, and surfaces can be turned on and off (interaction requires Adobe Acrobat version 7.0.8 or higher). In the printed version, the front face of each 3D cube (the 'home' view in the interactive online version) corresponds exactly to the patch of sky shown in Fig. 1, and velocity with respect to the Local Standard of Rest increases from front (-0.5 km s^{-1}) to back (8 km s^{-1}).

data, CLUMPFIND typically finds features on a limited range of scales, above but close to the physical resolution of the data, and its results can be overly dependent on input parameters. By tuning CLUMPFIND's two free parameters, the same molecular-line data set[8] can be used to show either that the frequency distribution of clump mass is the same as the initial mass function of stars or that it follows the much shallower mass function associated with large-scale molecular clouds (Supplementary Fig. 1).

Four years before the advent of CLUMPFIND, 'structure trees'[9] were proposed as a way to characterize clouds' hierarchical structure

using 2D maps of column density. With th…rly 2D work as inspiration, we have developed a structure-id…rithm that abstracts the hierarchical structure of a… an easily visualized representation calle… well developed in other data-intensive… application of tree methodologies so fa… and almost exclusively within the a… 'merger trees' are being used with in…

Figure 3 and its legend explain t…

These are "dead" panels! That's not good enough.

…mass, su… K^{-1} km^{-1} s… …ary Fig. 2). …can then be used to estimate the role of self-gravity at each point in the hierarchy, via calculation of an 'observed' virial parameter, $\alpha_{obs} = 5\sigma_v^2 R/GM_{lum}$. In principle, extended portions of the tree (Fig. 2, yellow highlighting) where $\alpha_{obs} < 2$ (where gravitational energy is comparable to or larger than kinetic energy) correspond to regions of p–p–v space where self-gravity is significant. As α_{obs} only represents the ratio of kinetic energy to gravitational energy at one point in time, and does not explicitly capture external over-pressure and/or magnetic fields[16], its measured value should only be used as a guide to the longevity (boundedness) of any particular feature.

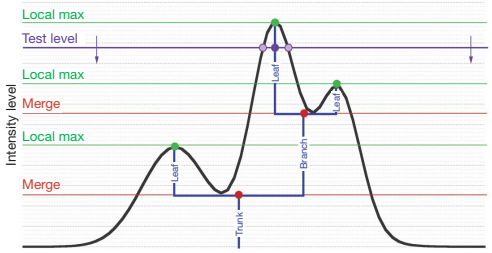

Figure 3 | Schematic illustration of the dendrogram process. Shown is the construction of a dendrogram from a hypothetical one-dimensional emission profile (black). The dendrogram (blue) can be constructed by 'dropping' a test constant emission level (purple) from above in tiny steps (exaggerated in size here, light lines) until all the local maxima and mergers are found, and connected as shown. The intersection of a test level with the emission is a set of points (for example the light purple dots) in one dimension, a planar curve in two dimensions, and an isosurface in three dimensions. The dendrogram of 3D data shown in Fig. 2c is the direct analogue of the tree shown here, only constructed from 'isosurface' rather than 'point' intersections. It has been sorted and flattened for representation on a flat page, as fully representing dendrograms for 3D data cubes would require four dimensions.

©2009 Macmillan Publishers Limited. All rights reserved

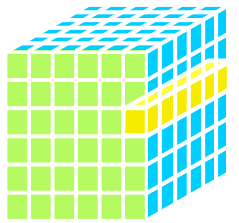

Goodman et al. 2009, Nature, cf: Fluke et al. 2009

Linked Views of High-dimensional Data

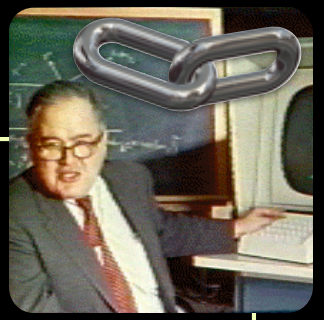

John Tukey

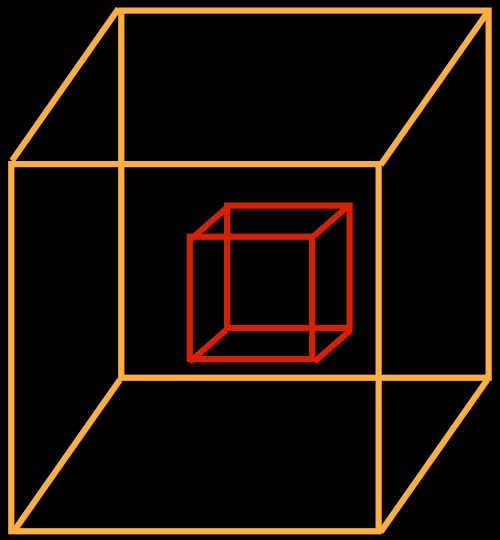

3D

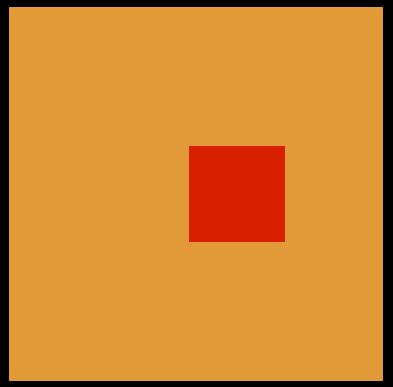

2D

Statistics

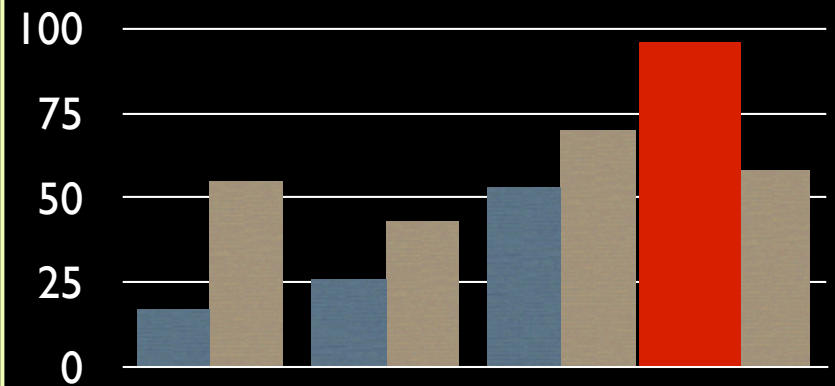

Data Abstraction

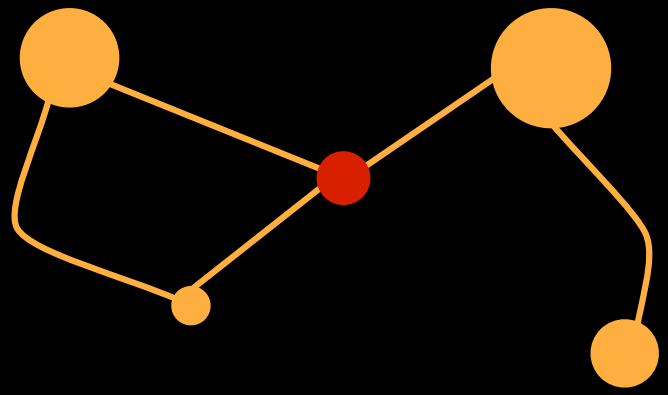

figure, by M. Borkin, reproduced from Goodman 2012, "Principles of High-Dimensional Data Visualization in Astronomy"

JOHN TUKEY'S LEGACY

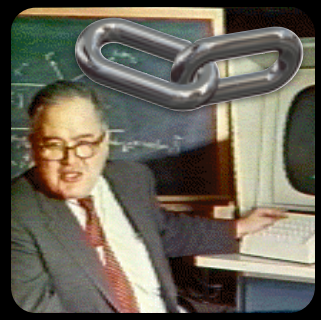

PRIM-9

PRIM-H

DataDesk®

glue

XGobi

GGobi

RGGobi

Spotfire®

Polaris

tableau SOFTWARE

1970 1980 1990 2000 2010

LINKED VIEWS OF HIGH-DIMENSIONAL DATA (IN PYTHON)

GLUE

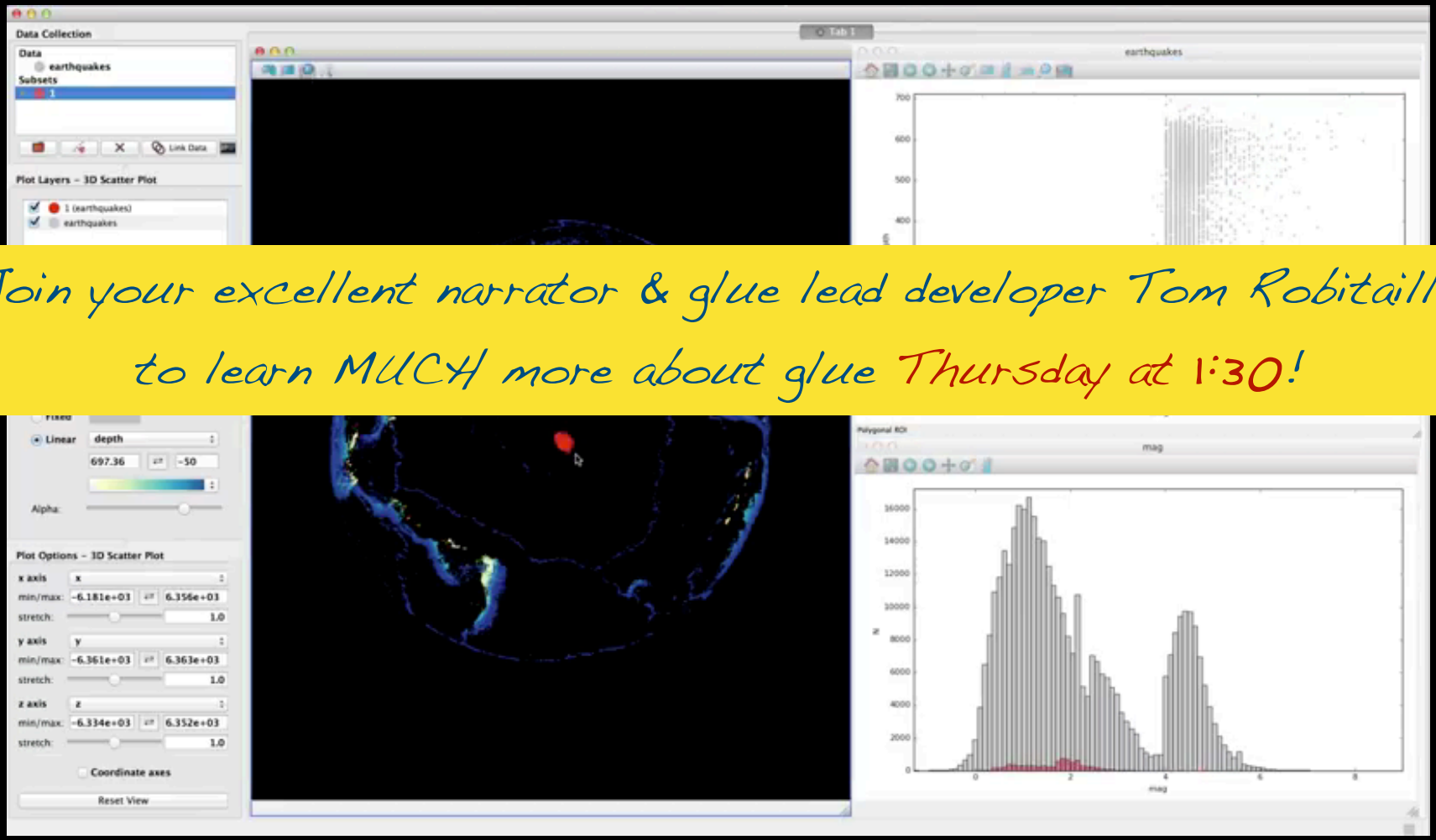

Join your excellent narrator & glue lead developer Tom Robitaille to learn MUCH more about glue Thursday at 1:30!

video by Tom Robitaille, lead glue developer

glue created by: C. Beaumont, M. Borkin, P. Qian, T. Robitaille, and A. Goodman, PI

LINKED VIEWS OF HIGH-DIMENSIONAL DATA (IN PYTHON)

GLUE

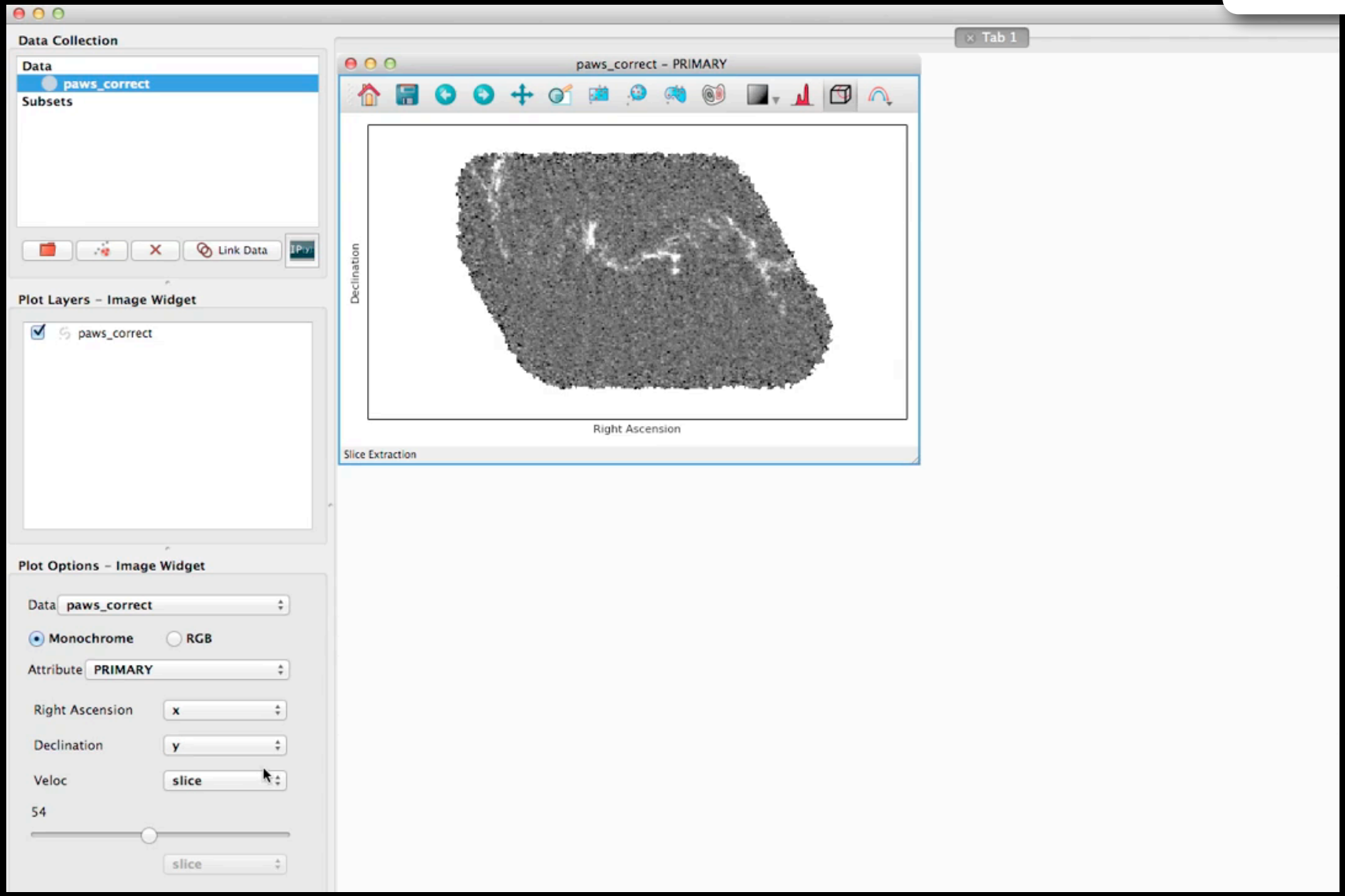

video by Chris Beaumont, glue developer

glue created by: C. Beaumont, M. Borkin, P. Qian, T. Robitaille, and A. Goodman, PI

glue

multidimensional data exploration

your handout

built-in

standard data loaders

Data File 1

Data File 2

Data File N

define new variables, import/export insights, interactive plots for the web, save state, all from GUI

standard 1D, 2D & 3D plots

link data files' attributes

highlight live or algorithmic selections with Boolean logic

plug-in

custom data loaders

custom buttons, features

custom plots

?

+options

user config.py file (loaders, colors, plot types, +)

access to all matplotlib functions through built-in IPython terminal

run & interact with glue from Jupyter notebook & other tools

glueviz.org

What is visualization (and all this software) for?

INSIGHT

CONTEXT	PATTERN RECOGNITION	EVALUATION
Spatial	Ideas	Algorithms
Non-Spatial	Outliers	Errors

“Is Nessie Parallel to the Galactic Plane?”

-A. Burkert, 2012

Celestial North

Yes but why not at Zero of Latitude ($b=0$)?

Where are we, really?

"IAU Milky Way", est. 1959

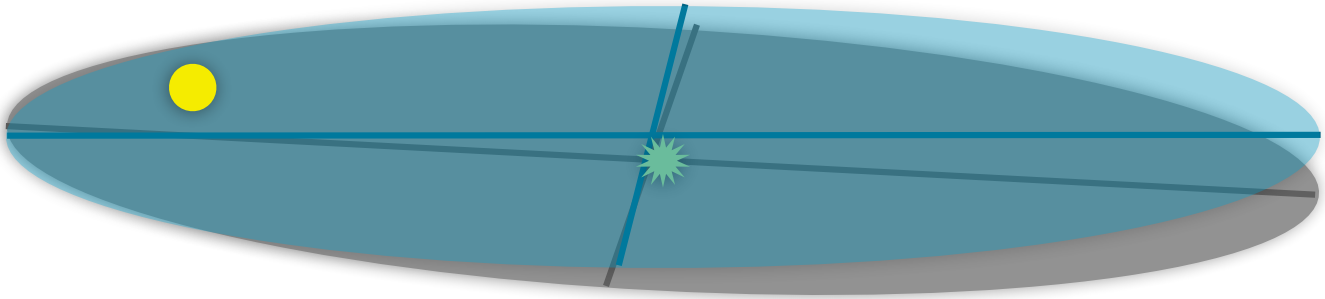

True Milky Way, modern

The equatorial plane of the new co-ordinate system must of necessity pass through the sun. It is a fortunate circumstance that, within the observational uncertainty, both the sun and Sagittarius A lie in the mean plane of the Galaxy as determined from the hydrogen observations. If the sun had not been so placed, points in the mean plane would not lie on the galactic equator. *[Blaauw et al. 1959]*

Sun is ~25 pc "above" the IAU Milky Way Plane

+

Galactic Center is ~7 pc offset from the IAU Milky Way Center

=

The **Galactic Plane is not quite where you'd think it is** when you look at the sky

In the plane! And at distance of spiral arm!

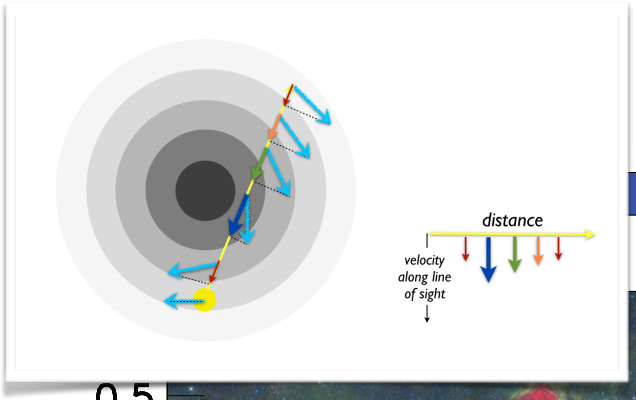

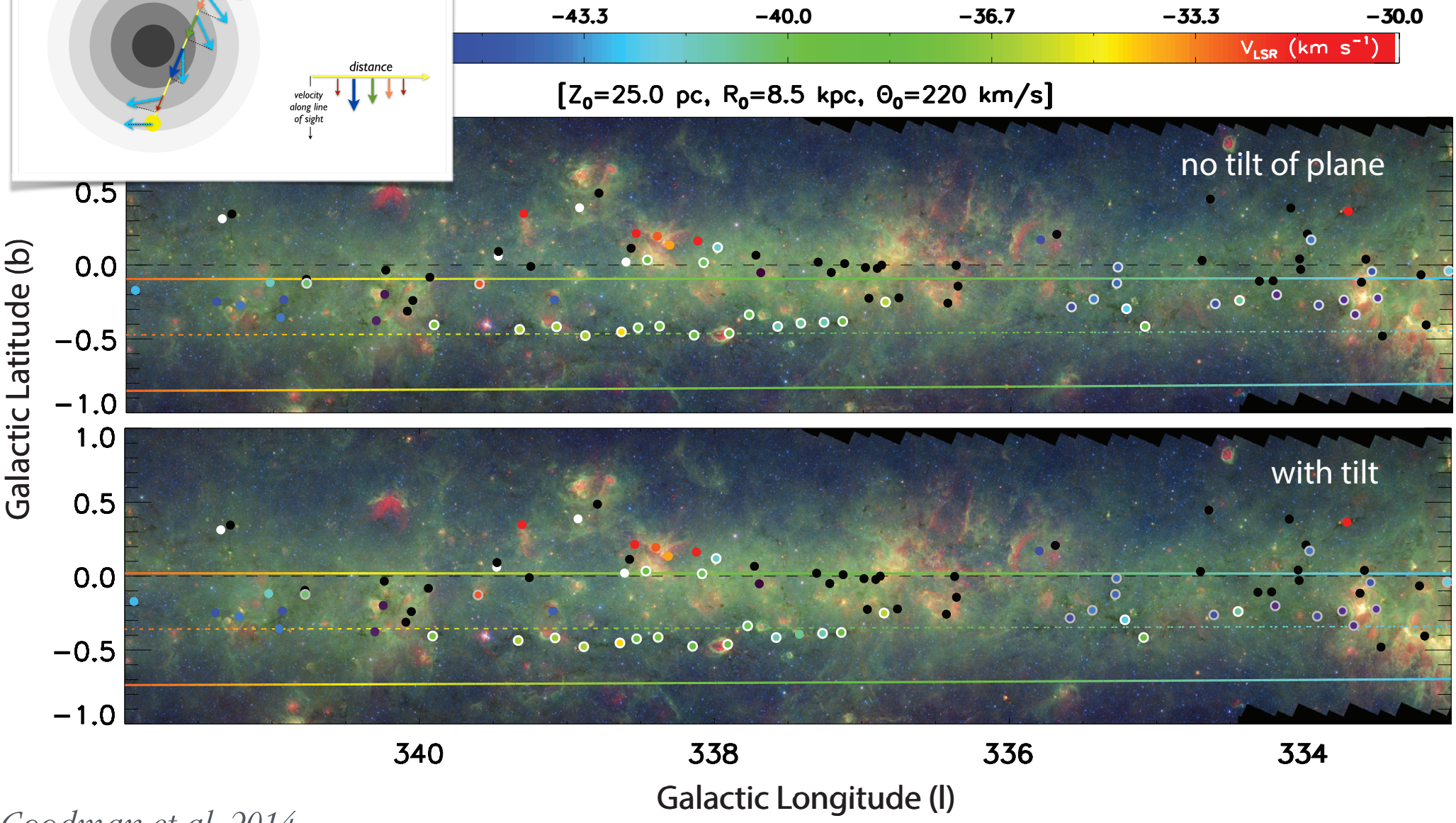

Goodman et al. 2014

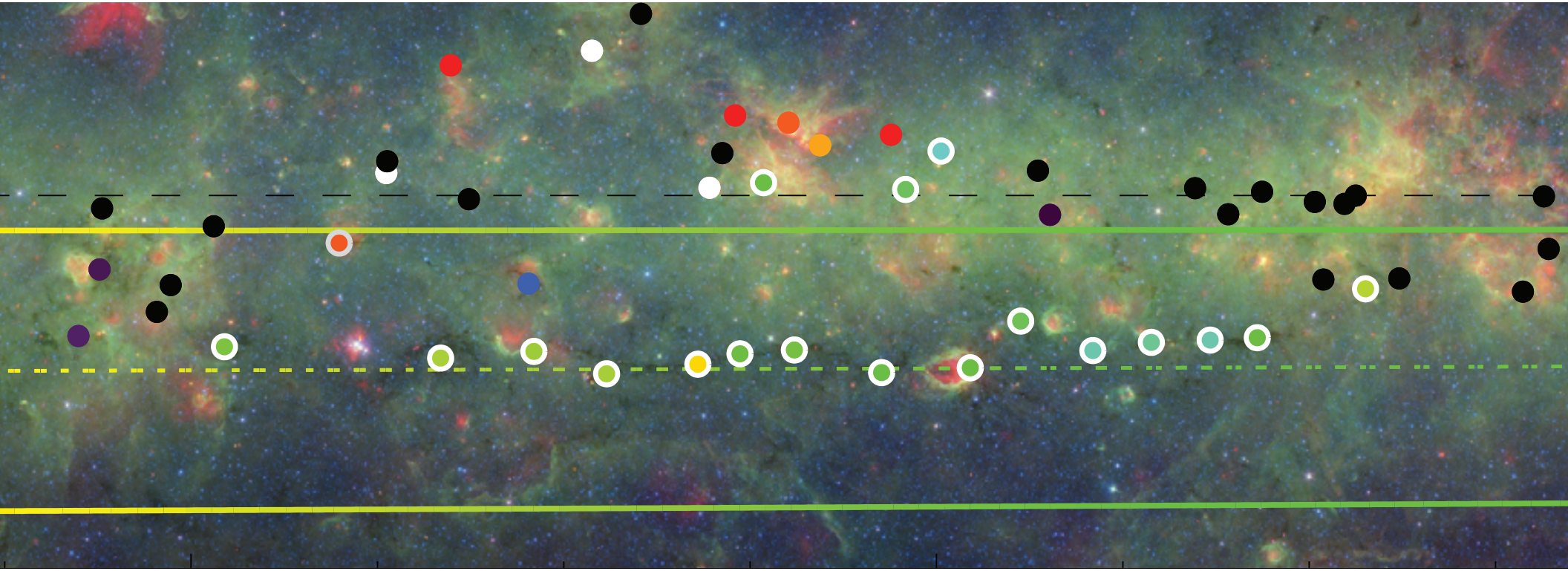

...eerily precisely...

Goodman et al. 2014

2014 Simulation

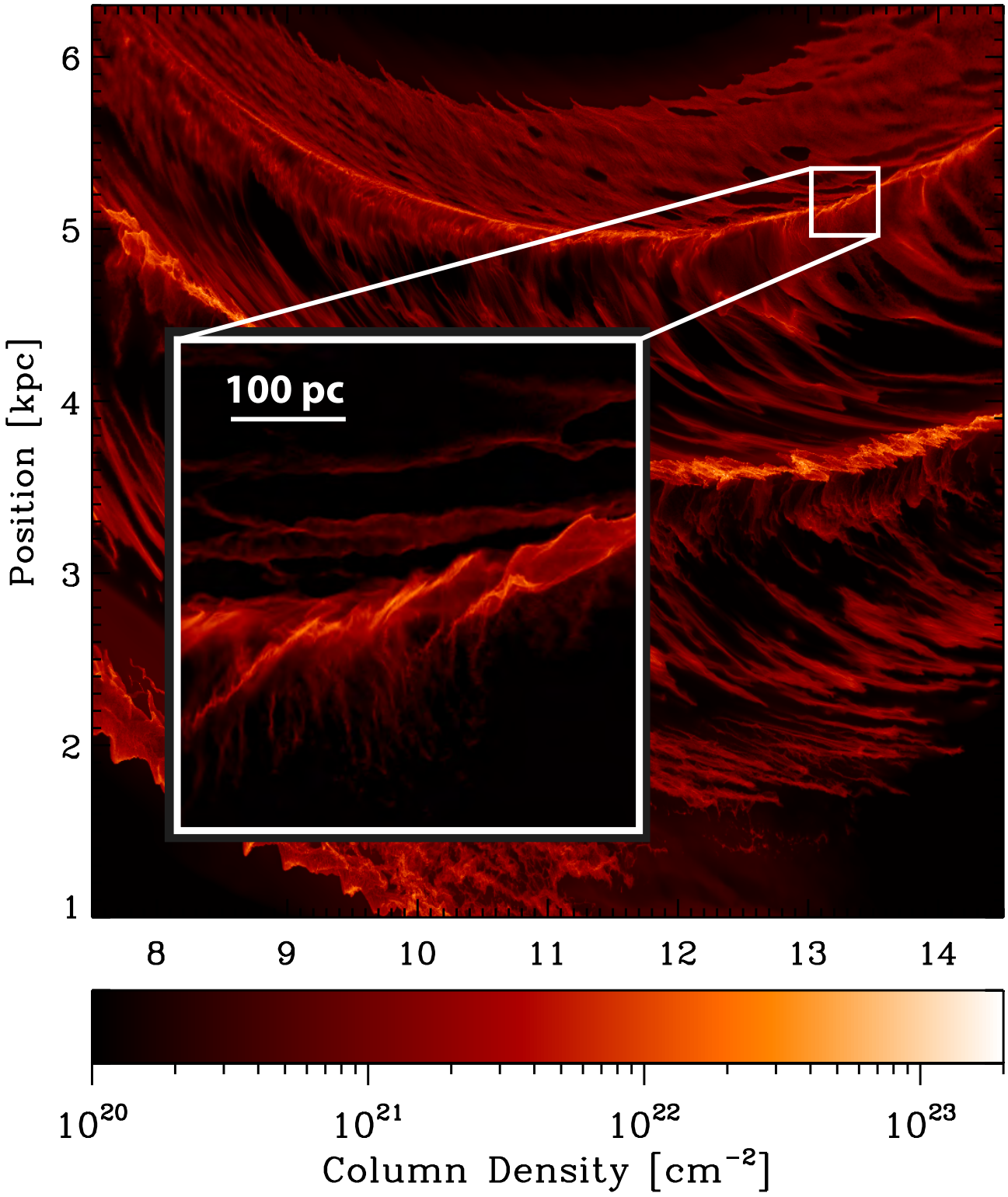

Smith et al. 2014, using AREPO

2014 Simulation

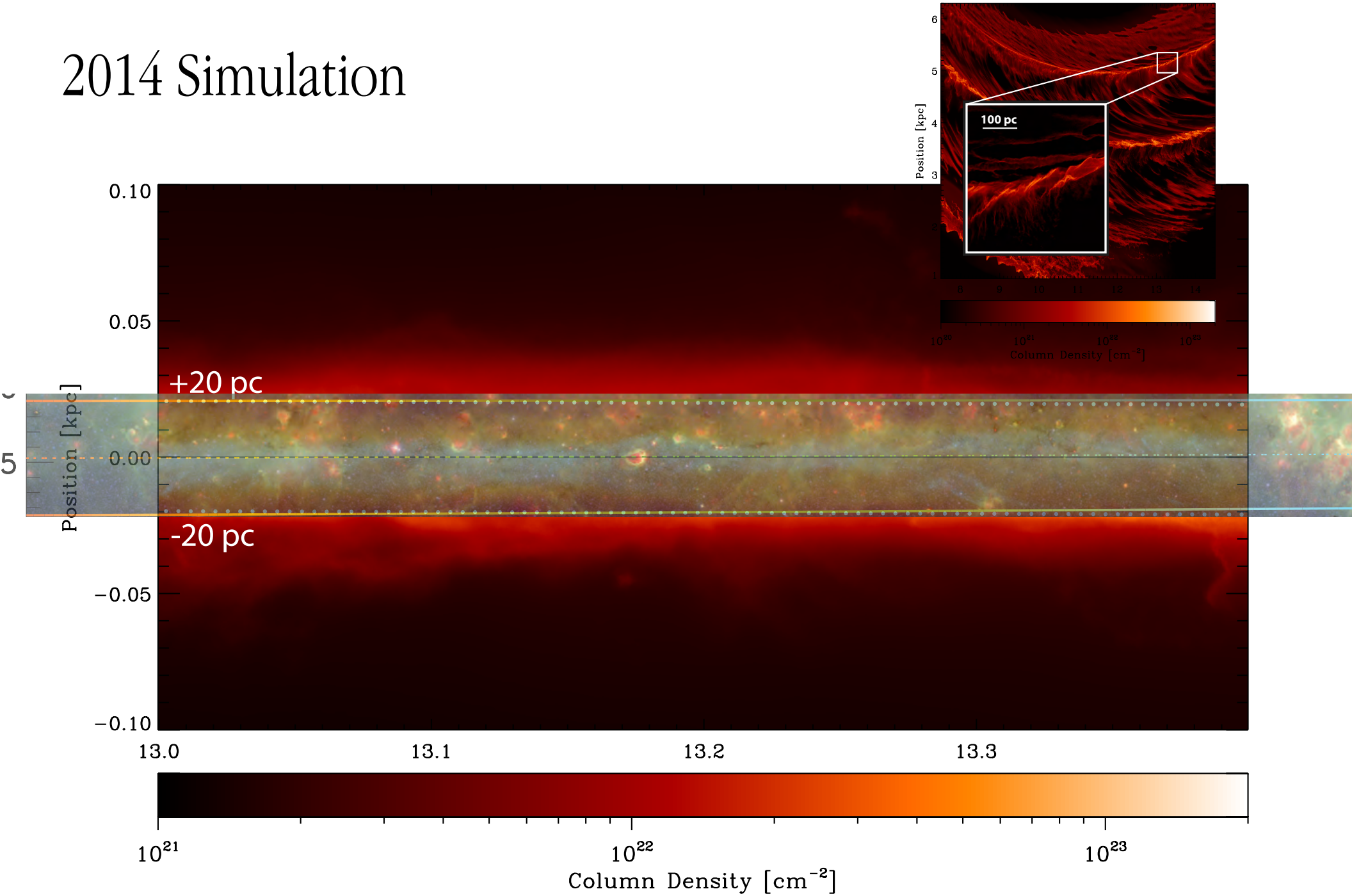

Smith et al. 2014, using AREPO (hydro+chemistry, imposed potential, no B-fields, no local (self-)gravity, no feedback)

NESSIE IN GLUE+WWT

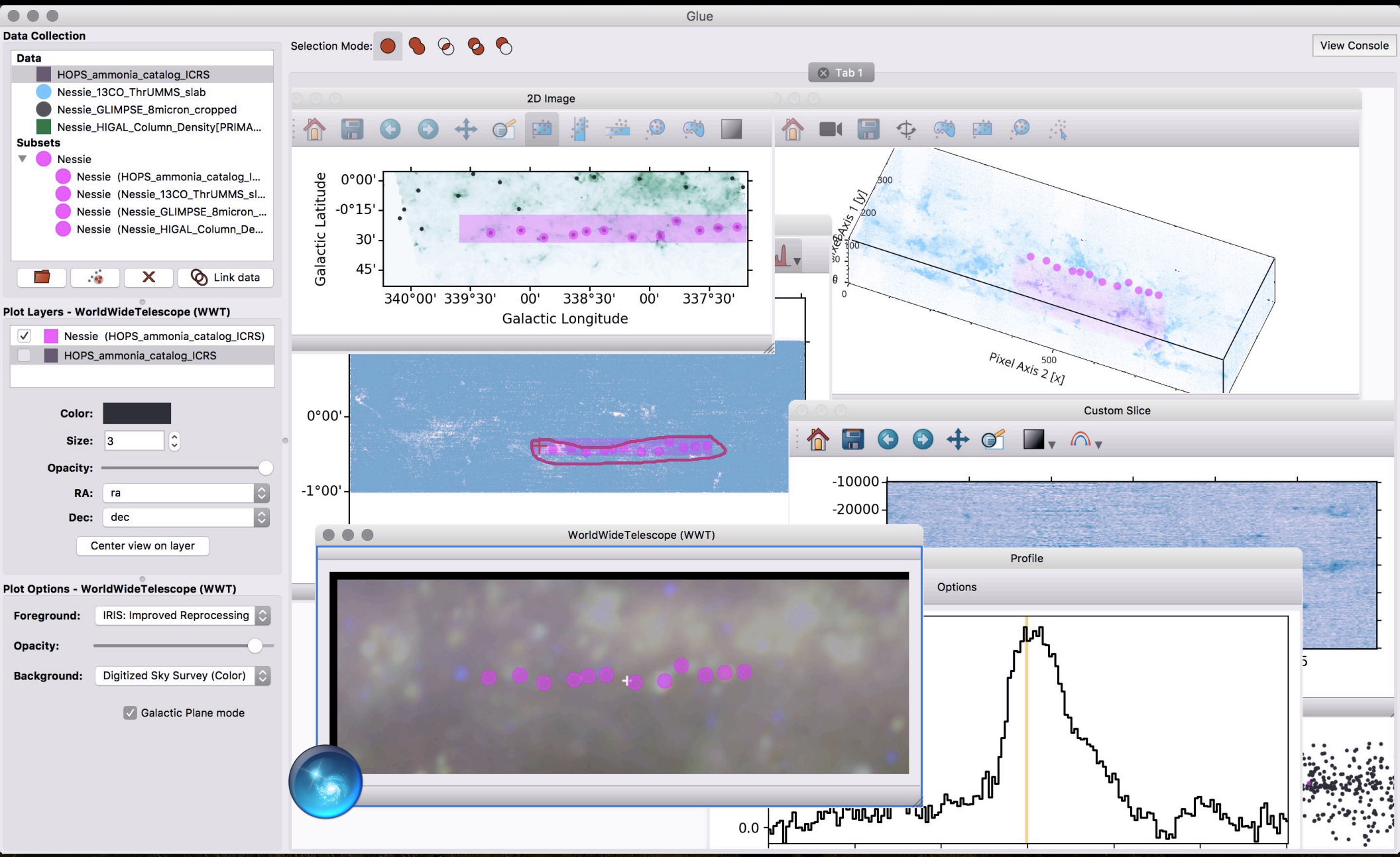

NESSIE IN GLUE+WWT

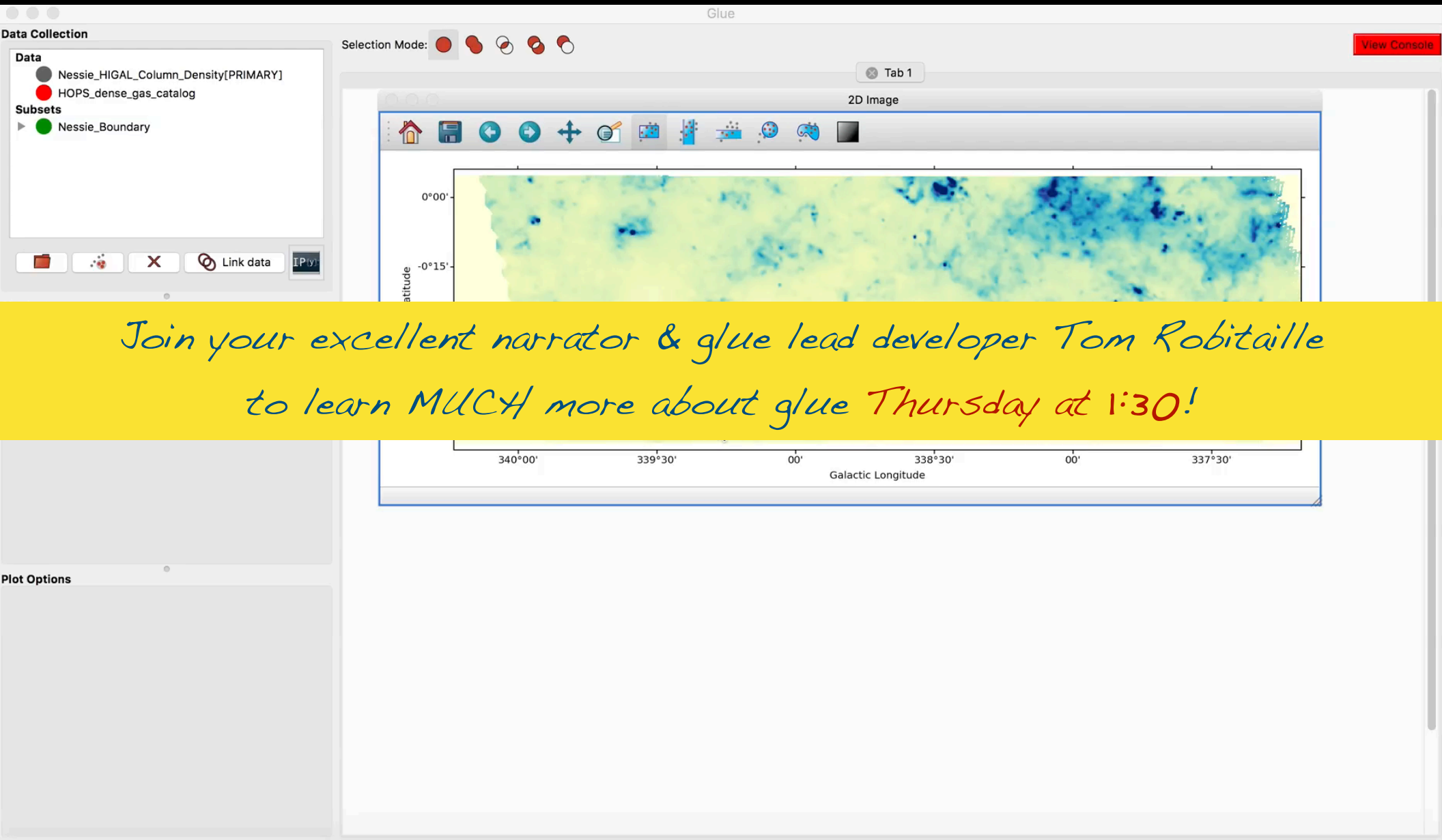

Join your excellent narrator & glue lead developer Tom Robitaille to learn MUCH more about glue Thursday at 1:30!

Big DATA
versus
Wide DATA

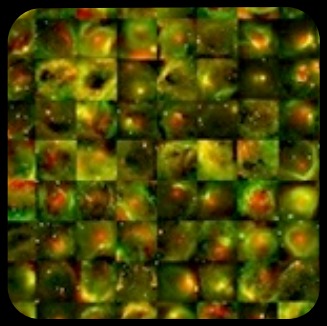

PHILOSOPHICAL
TRANSACTION

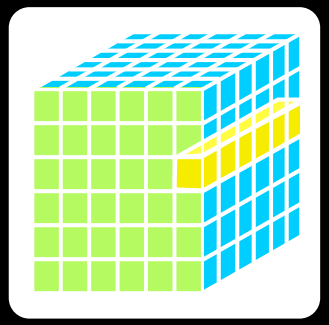

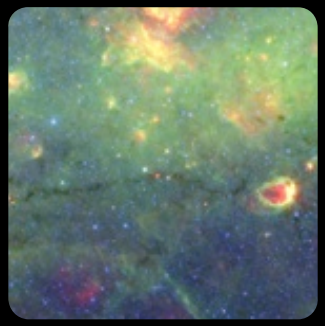

WorldWide Telescope

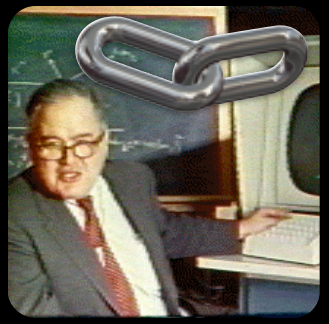

glue
multidimensional data exploration

ADS
ALL SKY
SURVEY

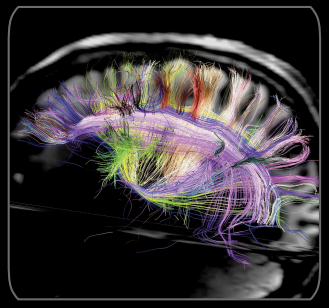

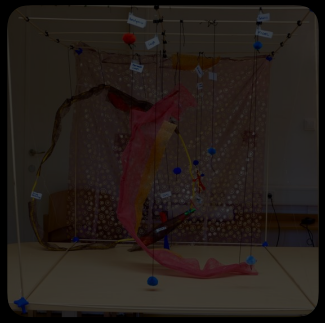

The challenge of 3D Selection

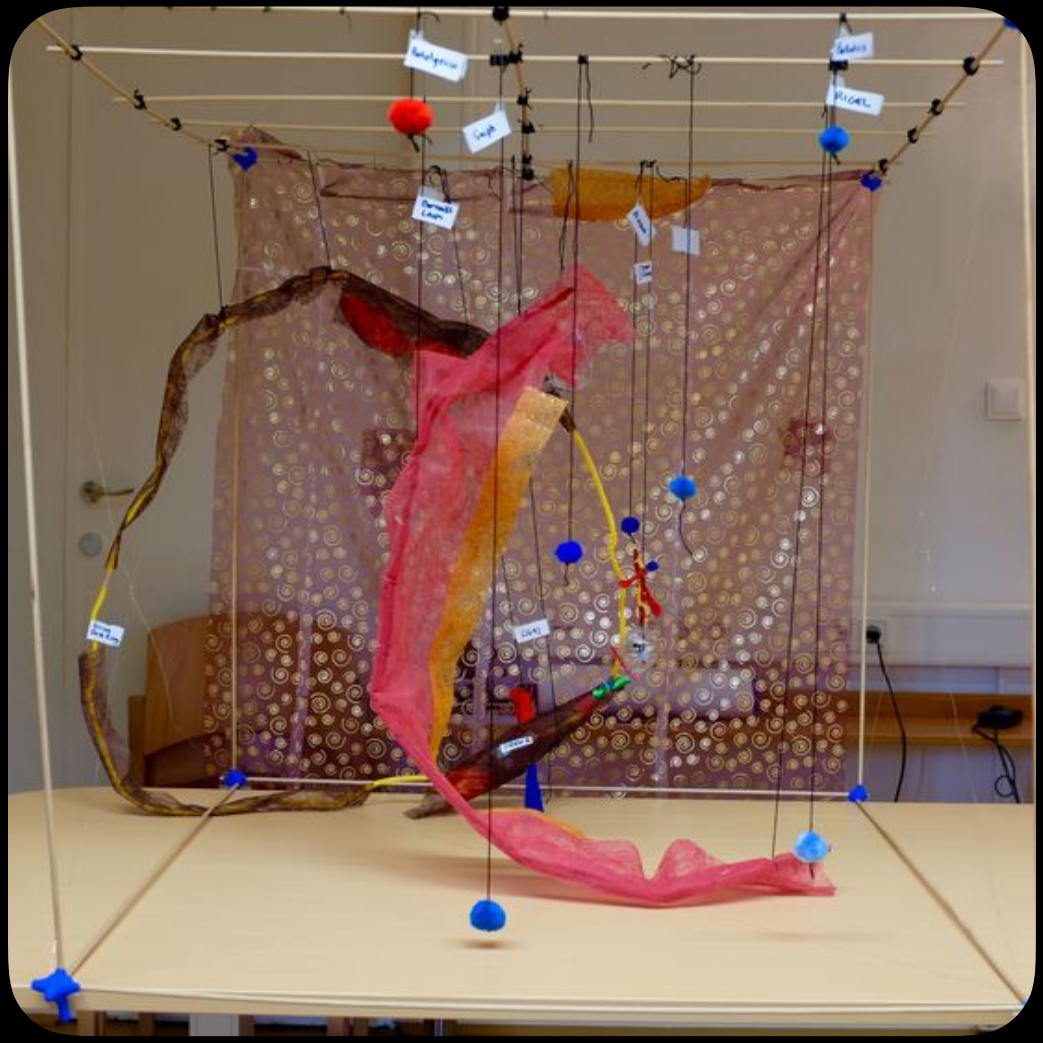

A state-of-the-art 3D model of the stars & gas near the Orion nebula, created at Orion (un)plugged, Vienna, 2015.
Expert builders (~20 total) include: Joao Alves, John Bally, Alyssa Goodman & Eddie Schlafly. (cf. "Image & Meaning" workshops by Felice Frankel)
YouTube video explanation; WWT Tour

The challenge of 3D Selection

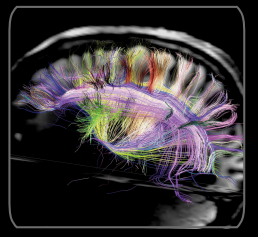

Viz-e-lab

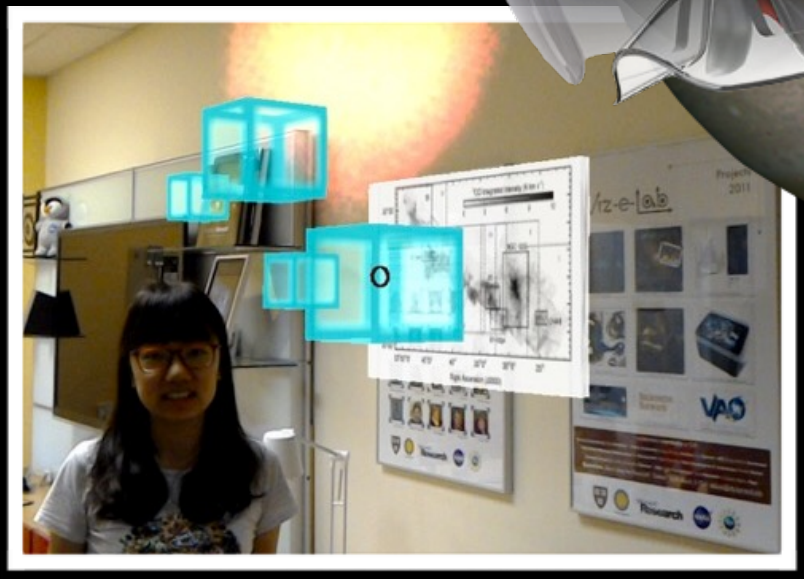

$$F = \frac{Gm_1m_2}{R^2}$$

Paper of the Future

Cognition

Language*

Data

Pictures

Communication

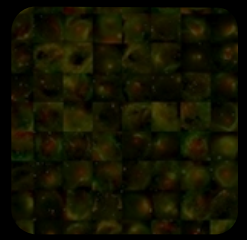

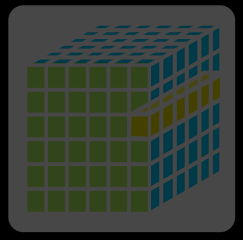

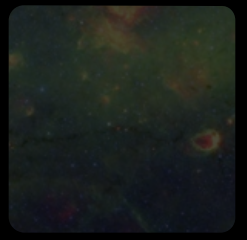

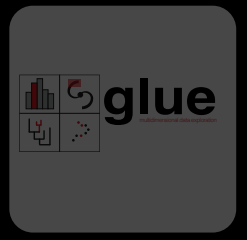

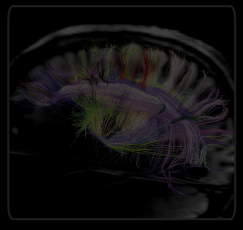

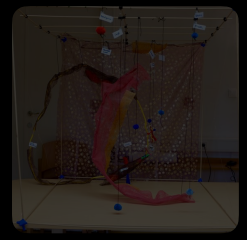

Literature as (a filter for) Data

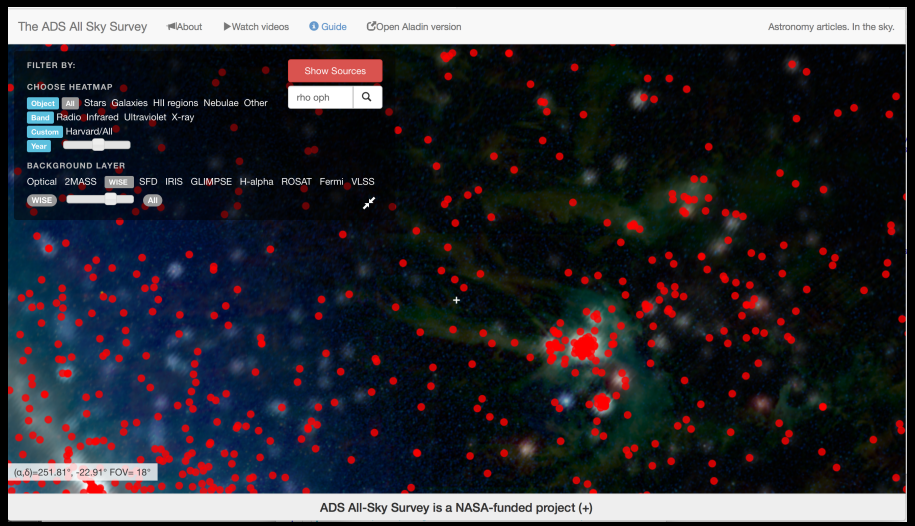

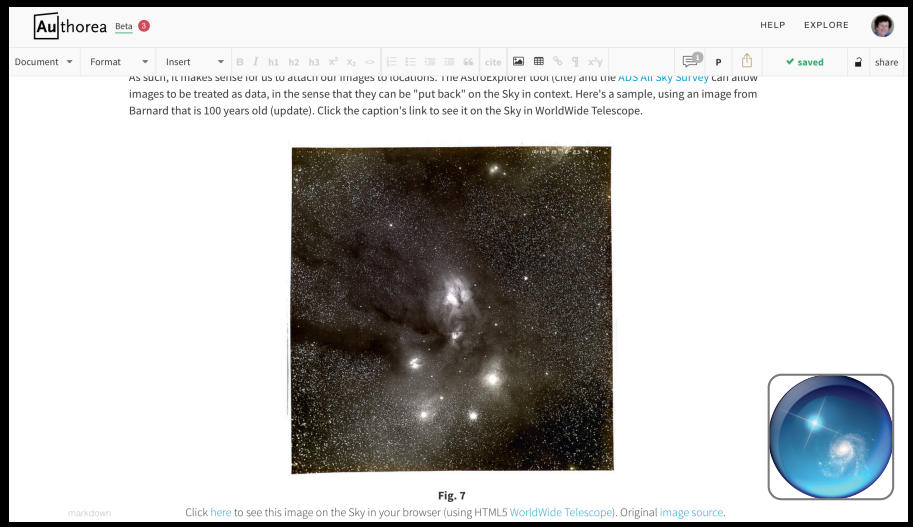

Many thanks to Alberto Pepe, August Muench, Thomas Boch, Jonathan Fay, Michael Kurtz, Alberto Accomazzi, Julie Steffen, Laura Trouille, David Hogg, Dustin Lang, Christopher Stumm, Chris Beaumont & Phil Rosenfield for making this all work!

ADS All-Sky Survey & Astronomy Rewind

"putting articles and images (back) on the Sky"

your handout

1. Images Extracted from Journal Articles

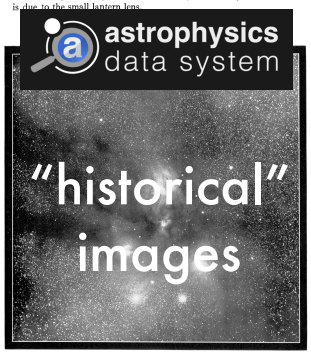

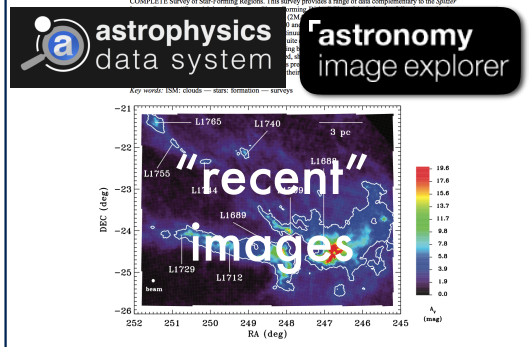

2. Missing coordinate metadata added back to images, either...

...automatically, applying astronometry.net to wide-field optical images, or

Astrometry.net

via "Astronomy Rewind" Zooniverse Citizen Science Project

ZOONIVERSE

3. "Solved" images returned to ADS & Astronomy Image Explorer

astrophysics data system

astronomy image explorer

4. New button in Astronomy Image Explorer offers image-in-context, using AAS' WorldWide Telescope in the browser

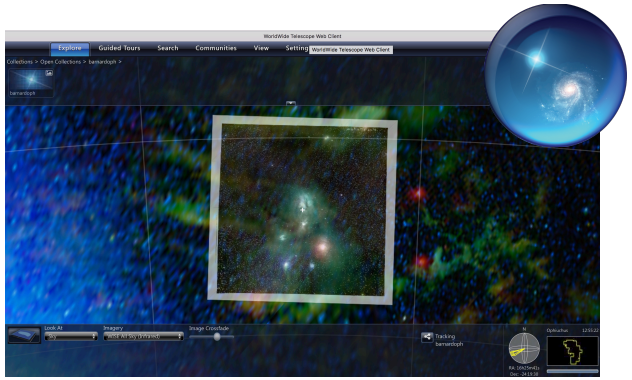

0. ADS All-Sky Survey

click entries on the timeline to try out services

ADS	WorldWide Telescope	Zooniverse	Astrometry.net	ADS All Sky Survey	Astronomy Image Explorer	Astronomy Rewind
1992	2008	2009	2011	2014	2014	2017

The Astronomical Journal, 131:2921–2933, 2006 June
© 2006. The American Astronomical Society. All rights reserved. Printed in U.S.A.

THE COMPLETE SURVEY OF STAR-FORMING REGIONS: PHASE I DATA

Naomi A. Ridge,[1] James Di Francesco,[2] Helen Kirk,[2,3] Di Li,[1,4] Alyssa A. Goodman,[1] João F. Alves,[5] Héctor G. Arce,[6] Michelle A. Borkin,[7] Paola Caselli,[8] Jonathan B. Foster,[1] Mark H. Heyer,[9] Doug Johnstone,[2,3] David A. Kosslyn,[1] Marco Lombardi,[4] Jaime E. Pineda,[1] Scott L. Schnee,[1] and Mario Tafalla[10]

Received 2005 November 8; accepted 2006 February 22

ABSTRACT

We present an overview of data available for the Ophiuchus and Perseus molecular clouds from Phase I of the COMPLETE Survey of Star-Forming Regions. This survey provides a range of data complementary to the *Spitzer* Legacy Program "From Molecular Cores to Planet Forming Disks." Phase I includes the following: extinction maps derived from the Two Micron All Sky Survey (2MASS) near-infrared data using the NICER algorithm; extinction and temperature maps derived from *IRAS* 60 and 100 μm emission; H I maps of atomic gas; ^{12}CO and ^{13}CO maps of molecular gas; and submillimeter continuum images of emission from dust in dense cores. Not unexpectedly, the morphology of the regions appears quite different depending on the column density tracer that is used, with *IRAS* tracing mainly warmer dust and CO being biased by chemical, excitation, and optical depth effects. Histograms of column density distribution are presented, showing that extinction as derived from 2MASS NICER gives the closest match to a lognormal distribution, as is predicted by numerical simulations. All the data presented in this paper, and links to more detailed publications on their implications, are publicly available at the COMPLETE Web site.

Key words: ISM: clouds — stars: formation — surveys

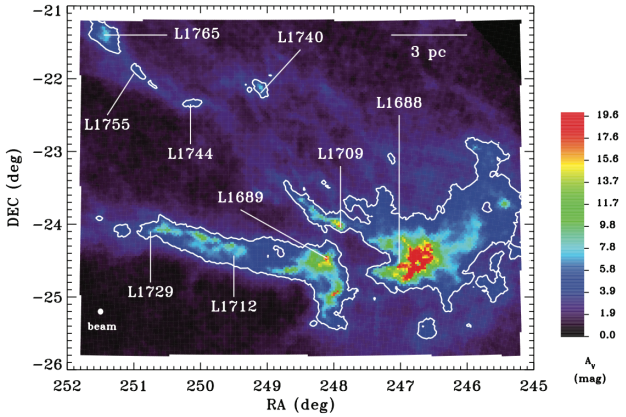

Fig. 3.—Map of extinction in Ophiuchus derived using 2MASS NICER. The contour indicates an A_V of 3 mag and is repeated in subsequent figures for orientation. Note that the small "hole" at the center of the L1688 cluster is an artifact due to the high extinction at that position.

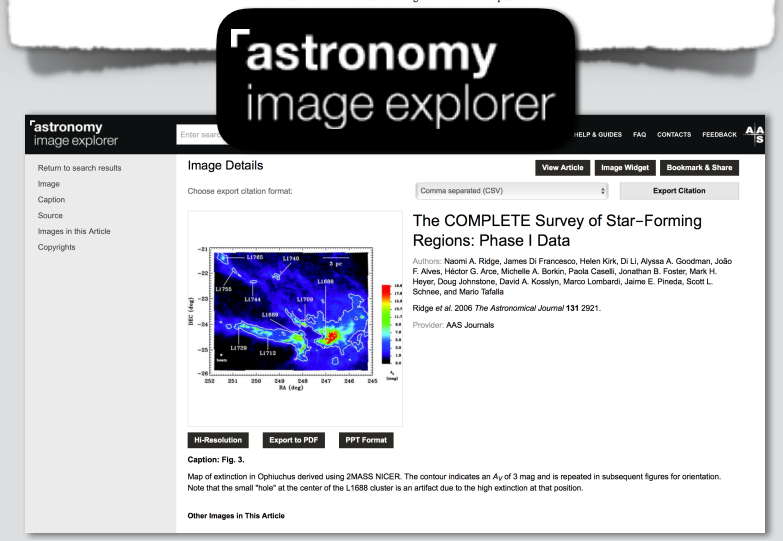

Who, How, and Who's Paying?

The **ADS All Sky Survey** was first funded via a 2012 grant from the **NASA ADAP** program to Seamless Astronomy, in collaboration with CDS, Astrometry.net and Microsoft Research.

Articles-on-the-Sky

was first deployed in 2014, using APIs from WWT (Microsoft Research, now AAS) and CDS (Aladin)

Images-on-the-Sky

relies on the astrometry.net, Zooniverse, IOP/AAS Astronomy Image Explorer and WorldWide Telescope platforms, and it is funded by the **American Astronomical Society**, in addition to the NASA ADAP grant.

These projects rely on open source sofware, primarily hosted on **GitHub**.

PI to contact for more information
Alyssa Goodman, Harvard
agoodman@cfa.harvard.edu

SEAMLESS ASTRONOMY
Linking scientific data, publications, and communities

your handout

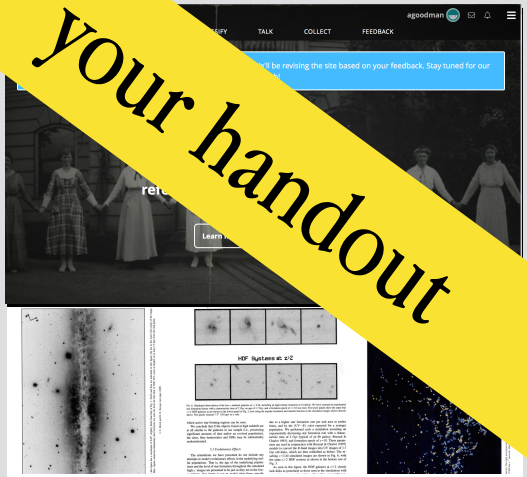

1 person is talking about **Astronomy Rewind** right now.

Join in

ASTRONOMY REWIND STATISTICS

100% Complete

201	1,987	360	360
Volunteers	Classifications	Subjects	Completed Subjects

WORDS FROM THE RESEARCHER

"Your contributions unlock the information from old astronomy journals. Thank you and enjoy the images!"

ABOUT ASTRONOMY REWIND

This project is part of an ongoing NASA-funded effort aimed at turning the SAO/NASA Astrophysics Data System (ADS) into a data resource. The result will be a database of astro-referenced images, i.e., images of the sky for which coordinates, orientation, and pixel scale will be publicly available through NASA data archives, the Astronomy Image Explorer, and World Wide Telescope, thanks to your help!

ADLER PLANETARIUM

ZOONIVERSE

Privacy Policy

Seeing the Sky

Visualization & Astronomers

Alyssa A. Goodman
Harvard Smithsonian Center for Astrophysics & Radcliffe Institute for Advanced Study
@aagie

HARVARD UNIVERSITY
Microsoft Research
NSF
SEAMLESS ASTRONOMY
Linking scientific data, publications, and communities
Authorea
NASA
AAS AMERICAN ASTRONOMICAL SOCIETY
Enhancing and sharing humanity's scientific understanding of the universe since 1899.

To continue the conversation…

10qviz.org with Arzu Çöltekin (beta 2017, release 2018)

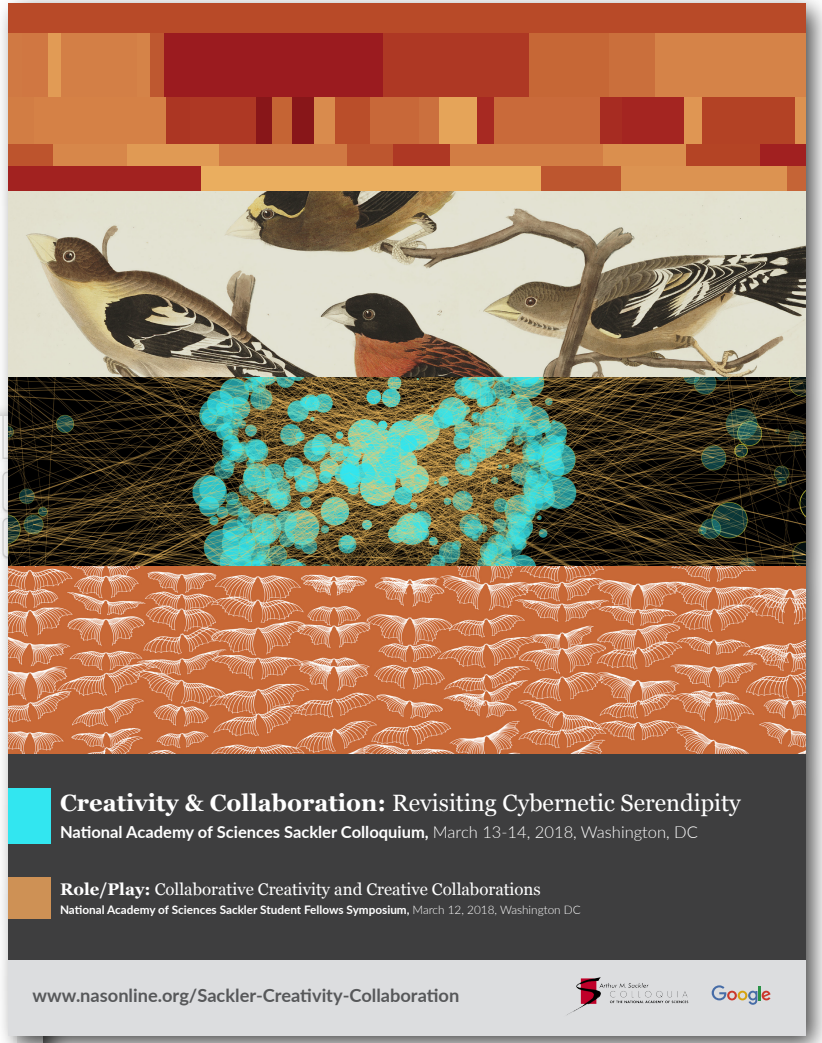

Creativity & Collaboration at NAS March 2018

with Ben Shneiderman, Maneesh Agrawala, Roger Malina, Youngmoo Kim & Donna Cox